Horst Dröscher

The chemical system of sodium acetate / water as phase change material (PCM) for the use in seasonal energy storage

Evaluation of stable settings in the chemical system of sodium acetate / water and advancement of a measuring method for determination of the enthalpy/temperature-characteristic during a storing cycle

DIPLOMARBEIT

zur Erlangung des akademischen Grades eines
Diplom-Ingenieurs

der Studienrichtung Chemieingenieurwesen
erreicht an der

Technischen Universität Graz

Siebenhofer, Matthäus, Univ.-Prof. Dipl.-Ing. Dr.techn.
Institut für Chemische Verfahrenstechnik und Umwelttechnik
Technische Universität Graz

Schranzhofer, Hermann, Dipl.-Ing. Dr.mont.
Institut für Wärmetechnik
Technische Universität Graz

2012

Eidesstattliche Erklärung

Ich erkläre an Eides statt, dass ich die vorliegende Arbeit selbstständig verfasst, andere als die angegebenen Quellen/Hilfsmittel nicht benutzt, und die den benutzten Quellen wörtlich und inhaltlich entnommenen Stellen als solche kenntlich gemacht habe.

Graz, am …… ……..

(Unterschrift)

STATUTORY DECLARATION

I declare that I have authored this thesis independently, that I have not used other than the declared sources / resources, and that I have explicitly marked all material which has been quoted either literally or by content from the used sources.

Graz, …… ……..

(Signature)

KURZFASSUNG

Titel: Das System Natriumacetat – Wasser als Phasenwechselmaterial zur saisonalen Wärmespeicherung

Autor: Horst Dröscher

1. Stichwort: Phasenwechselmaterial (PCM)
2. Stichwort: Natriumacetattrihydrat (SAT)
3. Stichwort: Materialeigenschaften

Wachsendes Bewusstsein in Klima- und Energiefragen führt zwingend zur Frage nach der zur Deckung des aktuellen Energiebedarfs verwendeten Energieträger. Ein großes Potential, fossile Rohstoffe durch erneuerbare Energieträger zu ersetzen, liegt in der Wärmebereitstellung mittels Solarthermie insbesondere im Gebäudebereich. Um hohe solare Deckungsgrade zu erreichen, ist es notwendig, die saisonale Verschiebung zwischen Wärmebedarf und Solar-Angebot mittels Wärmespeichern auszugleichen, wobei die wirtschaftliche Konkurrenzfähigkeit und gesellschaftliche Akzeptanz solcher Systeme wesentlich von der Kompaktheit der verwendeten Speicher abhängt.
Im EU-Projekt COMTES (Combined development of compact thermal energy storage technologies) sollen derartige kompakte Wärmespeicher entwickelt und realisiert werden. Eine Möglichkeit dazu bietet die Verwendung von Phasenwechselmaterialien (phase change material, PCM), im speziellen Natriumacetattriydrat (SAT), welches sich durch hohe Speicherdichten und die Möglichkeit der Unterkühlung der flüssigen Phase bis auf Raumtemperatur auszeichnet. Dadurch ist eine nahezu verlustfreie, langfristige (saisonale) Speicherung der Energie in Form von Phasenwechselenergie realisierbar; eine gezielte Auslösung der Kristallisation ermöglicht bei Bedarf die Abgabe der gespeicherten Energie.
Im Rahmen der vorliegenden Arbeit wurden Experimente mit SAT durchgeführt, um das Material insbesondere im unterkühlten Zustand charakterisieren zu können.
Das Phänomen der Segregation in der unterkühlten flüssigen Phase wurde untersucht, wobei sich eine Korrelation zwischen dem Ausmaß des Auftretens der Segregation und der Konzentration (Wasser/Natriumacetat) zeigte, ein eindeutiger Zusammenhang mit der Füllhöhe in Probenrohren konnte jedoch nicht nachgewiesen werden.
Möglichkeiten der gezielten Auslösung der Kristallisation der unterkühlten flüssigen Phase wurden in Theorie und Experiment bearbeitet, wobei zwei Methoden entwickelt und reproduzierbar durchgeführt werden konnten: Impfmechanismus mit SAT-Kristallen bzw. homogene Keimbildung durch lokale Kühlung mittels Peltier-Einheit.
Für im Projekt COMTES nachfolgende thermische Anlagensimulationen ist die Enthalpie/Temperatur-Charakteristik des Materials eine wesentliche Eingangsgröße, wobei in der Literatur dafür verfügbare Daten speziell für den Bereich der Unterkühlung nicht in ausreichendem Umfang vorhanden sind. Zu deren Ermittlung wurden Messungen nach dem Prinzip der "T-history"-Methode durchgeführt und ausgewertet. Die Ergebnisse liegen im Bereich der in der Literatur angegebenen Werte, lassen jedoch aufgrund der geringen Stichprobenanzahl keine Aussage über ihre Zuverlässigkeit zu.
Erkenntnisse aus den aktuellen Experimenten bilden die Grundlage für weitere Messungen mit einem verbesserten Versuchsaufbau.

ABSTRACT

Title:
The chemical system of sodium acetate / water as phase change material (PCM) for the use in seasonal energy storage

Author: Horst Dröscher

1st keyword: Phase change material (PCM)
2nd keyword: Sodium acetate trihydrate (SAT)
3rd keyword: Material characteristics

Increasing concerns about climate and energy issues lead inevitably to the question of how the actual energy demand is covered. A great potential to substitute fossil fuels with renewable energy sources lies in the heat supply with solar thermal energy, especially in the building sector. To reach high solar fractions in the heat supply, thermal energy storages (TES) are required to bridge the seasonal time shift between heat demand and availability of solar energy. However, economic competitiveness and societal acceptance of such systems is considerably a question of how compact these storages can be built.
In the scope of the EU-project COMTES (Combined development of compact thermal energy storage technologies) such compact TES shall be developed and realized. One possibility to achieve this is to use phase change material (PCM), in particular sodium acetate trihydrate (SAT) that stands out not only due to its high storage density but its ability to undercool in the liquid phase even to ambient temperature. This fact allows an almost lossless, long-term (seasonal) storage of the energy as heat of fusion; directed triggering of crystallisation offers thermal discharging of the TES on demand.
Within the scope of this work experiments with SAT were performed in order to characterise the material especially in the undercooled state.
The phenomenon of segregation in the undercooled fluid phase was examined whereas a correlation between the amount of segregation and the concentration (water / sodium acetate) was observed; however, a definite relation to the filling height in test tubes could not be proven.
Methods for triggering crystallisation of the undercooled fluid phase were evaluated in theory and experiments whereby two mechanisms were developed and could be conducted reproducibly: seeding with SAT-crystals and homogenous nucleation due to local cooling by means of a Peltier unit.
For the further use within the project COMTES in thermal system simulation the enthalpy/temperature-characteristic of the material is a crucial input parameter wherefore quality of data available in literature is not satisfying especially for the undercooled phase. To gather more of this data measurements according to the "T-history"-method were carried out and evaluated. The results are in the range of the values from literature, though the number of samples was too small to allow for rating the result's reliability.
Observations and conclusions from the performed experiments establish a basis for further measurements with improved experimental setup.

Thanks to my family, my friends and most of all to my wife.

Whether you like it or not: physics always applies
- Anonymous -

Ever tried. Ever failed.No matter.
Try again. Fail again. Fail better
- Samuel Beckett -

CONTENT

1 INTRODUCTION

Energy distribution is a question of management [1]. To do this in a proper way it needs plenty of knowledge in a wide field of expertise. One is natural science, with its aim to understand and describe natural effects, in order to use this knowledge in any every day process e.g. energy supply. Talking about energy, its two characteristics quantity and quality are often used. Two basic concepts of physics, the first and the second law of thermodynamics are capable to describe the two main characteristics of energy, its quantity and quality.

The quantity is the amount of energy e.g. to heat a given amount of water from ambient temperature to a higher temperature a certain amount of energy is used but it is not lost, it is stored in the water. It is common knowledge that energy cannot be destroyed nor produced. The amount of energy is conserved which is the statement of the first law of thermodynamics. To get a sense for the quality of energy one has to think about the second law of thermodynamics. It states, that any process that happens in a closed system in a spontaneous way, increases the entropy of the system. With a process that happens in a spontaneous way is meant, that the process happens without doing any additional work like the cooling of hot water. For the inverse process like cooling in a refrigerator work is needed to drive the process. Entropy is generally known as a measure for disorder. The thermodynamic definition of entropy S describes the change of entropy during the change between two states of a system. The entropy change dS during a change of a system between two states in a process is defined as the reversible heat exchange dQ_{rev}, divided by the temperature T at which the heat is exchanged, $dS = dQ_{rev} / T$. A nice example to illustrate this concept is the cooling of water. If one considers a big pot of boiling water it is common sense that a loss of heat to the ambient arises. In fact the same amount of heat which is lost from the pot is transferred to the surrounding but not lost. It's appropriate to assume constant temperatures for both reservoirs if the transferred amount of heat is not to large. On calculating the entropy change dS for both systems out of the relation given above one will see that the loss of entropy from the pot is much smaller than the rise of entropy in the surrounding because the same amount of energy is divided by a big and a small temperature respectively. Thus the sum of entropy change is bigger than zero and the entropy of the whole system during the process of cooling has increased, like stated by the second law of thermodynamics. Daily experience tells us that the heating of a teapot out of the surrounding would never happen in a spontaneous fashion. This would be the reversal of cooling and it would result in a lowering of entropy which is thermodynamically forbidden for a spontaneous process. We can summarise, the same amount of heat in a state of high temperature has lower entropy than in a state of low temperature. Out of the knowledge that we are only able to use heat energy at sufficient high temperature to heat up a teapot entropy is a measure for quality of energy. The higher the temperature at which heat is supplied, the higher is the quality of energy. Burning fossil fuels can be done at very high temperature which means they are a high quality energy source.

To bring it back to energy supply and management of it, one needs to concern about the amounts of energy that are needed on a certain level of quality. Both can be estimated out of statistics of energy consumption. In figure 1-1 the total energy consumption of the

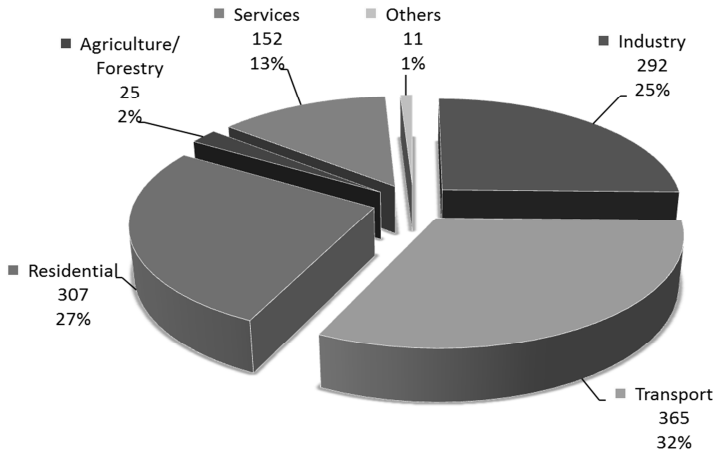

Figure 1-1: Final energy consumption of the 27 EU countries in 2010 by sector in 1000 tonnes of oil equivalent and percentage, respectively [2].

27 European Union (EU) countries in 2010 is depicted by sectors of consuming. The built environment is formed from more or less two sectors, services and residential. They covered together about 40% of the final energy consumption. Those two fields are interesting because all the others are either unknown (others, only 1%) or can be assumed to be high quality energy consumers (industry, transport, agriculture). But within the field of built environment it can be expected that different qualities of energy are consumed. A distribution for residential buildings by terms of energy use is shown in figure 1-2.

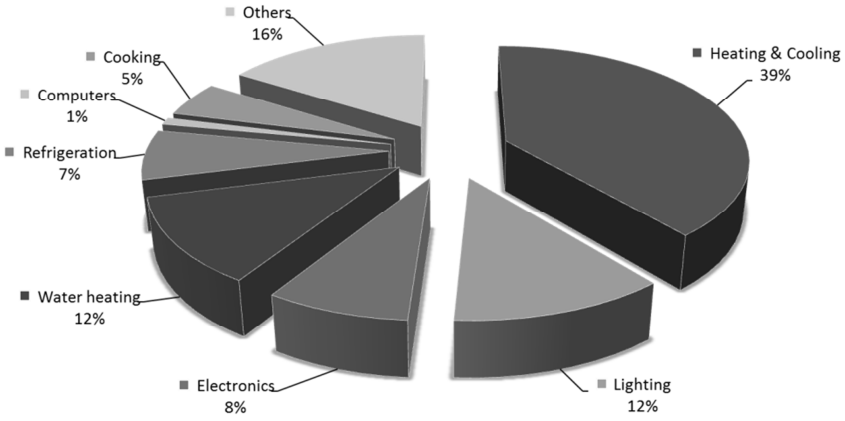

Figure 1-2: Distribution of energy in terms of use for residual buildings [3].

Fields with low quality energy demand should be heating & cooling and water heating – domestic hot water and space heating requires energy at temperatures of not higher than about 60 °C, which is very low quality compared to electricity where very high temperatures can be reached e.g. in an electric resistance of a furnace (more than 1200 °C). The low quality energy areas account together for around 50% of all the energy use in residential buildings. Thus for a rough estimation of final energy needed on a low quality level we

multiply the fraction of 40% for the built environment from the final energy consumption with the 50% for heat energy supply within the area of residential buildings. Sure, for a more exact estimation one would have to separate the different fields carefully in detail but roughly the multiplication above gives an estimation of 20% of the final energy consumption being low quality energy. Today still a huge amount of primary energy, e.g. fossil fuels which are high quality energy as mentioned above, is used to supply energy of a low quality level. In a last step an estimation of use in renewable energy could be done to get a sense for the remaining amount of primary energy used in the end to supply low quality energy. The share of renewable energy in final energy consumption for the year 2010 is given by the EU with 12.5% [4]. Merging the 12.5% with the 20% above the resulting estimation gives a potential of roughly 18% of primary energy that could be saved if low quality energy supply would be done in a perfect manner.
Recent developments in economy, general concern about limited fossil fuels and climate change forced the EU to programs like the Energy-efficient Buildings (EeB) Public Private Partnership (PPP) [3]. The goal of this program is to reduce the energy footprint and CO_2 emissions within the construction sector related to new and renovated buildings. The vision and focus of this program is to reduce the mentioned 18% of primary energy, used nowadays in a not very smart manner for heat supply in the housing, to zero by 2050 – it has to be mentioned that this program goes beyond heat energy but the other areas of energy supply in housing are not relevant for this work. There are plenty of ideas how to achieve these goals. But the need of multidisciplinary research in areas like demand reduction, renewable energy production and energy storage are named in the first place. One project sponsored by the EU, COMTES (Combined development of compact thermal energy storage technologies: project number 295568), fits within this scope of research. A brief description of COMTES and how this thesis is implemented in the project follows.

1.1 Motivation

In order to achieve the very ambitious vision of the EU of energy neutral buildings with zero emission by 2050 there can be two main strategies considered as mentioned above. Demand reduction on one hand and substitution of needed energy by means of e.g. renewable sources or industrial waste heat on the other. Substitution implies the problem to deal the area of conflict between demand and supply in terms of time. The chronological sequence of offer of industrial waste heat is depended on the processes that are carried out and is not capable to get aligned with heat demand for housing. The same applies to solar heat as renewable source. In winter where a lot of thermal energy is needed the offer of thermal energy is low and vice versa in summer. But not only in seasonal terms, also variation of demand during a daily cycle is not constant and is likely to be not aligned with the energy supply that is offered by the sun. This gap can be bridged by thermal energy storages (TES) – one field of research named within the EeB PPP.
TES have a long tradition in engineering and served always to smooth the gaps between demand and supply of heat energy. TES in the field of solar heating for residential buildings are state of the art, in both domestic hot water supply and also combined systems (domestic

hot water and space heating supply) [5]. For a heat supply of 100% solar fraction it is still challenging to build a TES because it has to be able to store the heat demand for a whole year. Storages that are capable to fulfil this requirement are called seasonal thermal energy storages.

Estimations weather the goal of 100% solar fraction could be reached have been done at the University of Denmark [6]. Seasonal storage by means of water tanks would require a volume of 40 – 50 m^3 for a family house which makes this solution rather inconvenient. A promising solution in order to reduce the size of a seasonal TES is to use materials with enhanced energy density. One type of materials with enhanced storage density are phase change materials (PCM). The estimations mentioned show, that a seasonal TES with PCM could be only 6 m^3 of volume in a Danish climate within certain boundary conditions.

This materials use besides the sensible heat (heat that results in temperature change of an object when exchanged and therefore can be sensed directly) the latent heat (latent is Latin for hidden and means that exchange of heat does not result in a change of temperature) of their phase change to increase their energy density. It's evident that the temperature of phase change has to be within the interesting temperature interval of the stored heat. Since the phase change of liquid to vapour would result in a huge volume change most of the used materials change between their solid and liquid state. Investigations on PCM's have been carried out for many years. One common property of a lot of those materials is to undercool (supercool). That means after melting followed by cooling below their melting point they do not go back to their solid state. Instead they stay liquid. For a long time this was considered as a problem, because undercooling was thought to be almost unpredictable and if the system undercools the latent heat stored in the material was trapped within the material. That is why nucleating agents are used in PCM to ensure a start of the crystallisation process.

Recent efforts try to use the effect of undercooling in a controlled way in order to get stable undercooled liquids. This makes it possible to withdraw sensible heat from the undercooling storage material after heating it above the melting point to use it for heat supply. Afterwards, when the storage has reached ambient temperature, the captured latent heat can be stored without heat loss. This is a huge advantage compared to e.g. water, which makes use of sensible heat only and can therefore not be used as storage material for heat energy without loss. The latent heat is then withdrawn from the undercooled liquid on demand by controlled solidification. This novel concept of undercooling should be carried out within the project COMTES.

COMTES is not only about PCM but more general about development and demonstration of three systems that are able to store solar thermal energy in compact seasonal storages in a significantly better way than water based systems do. This will enlarge the share of solar thermal energy within domestic energy demand. Besides undercooling PCM, solid sorption and liquid sorption form the three development lines.

The strength of this approach of collaboration is the synergy in working fields that overlap in the three development lines, without the risk of exchange of confidential data.

The field of tasks for the project is wide and starts with a definition of system boundary conditions and target applications. Investigations on best available storage materials for each line are followed by detailed numerical modelling of the physical processes and experimental

validation of these models to obtain an optimum component design. Process design is done by simulation, building full-scale prototypes and testing in the laboratory. Target of the whole project is an integrated evaluation of the systems and the potential based on one year of full monitoring in demonstration buildings. Involved industry partners are able to pick up the developed storage concepts in order to bring them to a commercial level.
In the project COMTES, for the first time, all relevant research disciplines of key scientific institutions in the fields of the three heat storage technologies work together in an international effort, assisted by a top-leading industry partner in each development line that contributes know-how and experience. COMTES provides the basis for further industrial development and the exploitation of the project results.

1.2 Aim of work

Since this thesis was written within a project at its start, the well-founded knowledge at the Institute of Thermal Engineering (IWT) was mixed with a bunch of observations and perceptions. In the following I try to give all the basic information about the investigated storage system related to this work that was available within the project partners. I've concentrated this knowledge during my work and it should give an overview of the setting of problems that should be treated within this work.
The decision for the used PCM, sodium acetate trihydrate (SAT), has been done at the very first beginning of the project, because a good knowledge base was available within our Danish partners [6], [7], [8]. But there was still missing information at the beginning of my work. Coming back to the chosen material, the idea was to use SAT in the very first beginnings of investigations at the Danish laboratories. To avoid problems of a phenomenon that occurred during cooling of SAT, called phase separation, the so called extra water principle was suggested. Therefore the used system is not the stoichiometric crystal SAT but a sodium acetate (SA)/water mixture. It seems that the problem of separation is still not solved and additional melting to liquids without crystals seems to be not entirely cleared.
Another crucial point is triggering crystallisation in an undercooled SA solution. Even though a lot of suggestions in literature are available a reliable method for triggering crystallisation is not defined within the project.
As mentioned above, numerical simulation should be done within the project to do optimisation work for component and process design. A still missing input is the enthalpy/temperature–progress (h/T-progress) during a cycle of the storage in a sufficient accurate way. This progress is dependent on the exact composition of the SA/water mixture and should therefore help to define the mixture that will be used in the storage. A method, the so called Temperature History Method (T-History-Method), to measure such curves has been used at the IWT for SAT without undercooling before. This method should be adapted for the measurement.
Another point to mention is that obviously the range of values for the heat capacity at constant pressure (c_p) and the phase change enthalpy of fusion ($\Delta_{fus}h$) in literature vary in a range that is too wide for proper simulation. An assumption to explain this variation is that different amounts of phase separation during the measurements at different institutions have

performed and caused these inaccuracies. Another assumption connected to the amount of phase separation is, that the amount of phase separation increases with the filling height of the investigated mixture within a container.
Out of these perceptions another step within the whole project has been done - the basic storage design. As mentioned above for a Danish family house a storage volume of 6 m^3 would be needed to fulfil the criterion of 100% solar fraction. It's a logistic problem to deal the heat release of the stored energy in winter in a practical way. The basic approach is to divide the whole volume into subunits that are able to deliver a certain manageable amount of energy in one step after controlled crystallisation. These subunits should be flat reservoirs that contain the storage material because of the separation issue. To find out if the filling height in such a storage module influences the storage capacity experiments with different filling heights should be done at the laboratory of the IWT in Graz.
Summarising there is a lot of knowledge but some points remain unsettled. The attempt of this work is to relate observations like melting problems and the problem of phase separation to thermodynamic parameters. The adaption of the T-History-Method for measurements with undercooling systems is investigated. This results in the need of finding a method to trigger crystallisation in a controlled way.
The introduction will now proceed with a collection of published data for c_p and $\Delta_{fus}h$.

1.3 Literature data for c_p and $\Delta_{fus}h$

The values for c_p and $\Delta_{fus}h$ in literature vary in a wide range and are given almost only for different compositions of mixtures. Thus a comparison of values from different sources gets difficult. This chapter gives a summary of collected data during my work. The given values represent published values from different sources that are known within the project partners. If available, short descriptions of measurements that lead to the values in this summary are given. This summary should underline the need of measurements to gain reliable h/T-curves for further processing in numerical calculations within the project COMTES.

Furbo published a value for $\Delta_{fus}h$ = 265 · kJ · kg^{-1} for SAT [7]. [Note HD: Most likely out of literature.]

Fan collected quantities of c_p for a solution of 58 wt% SA [8]. c_p is given in J · kg^{-1} · K^{-1} and T is in Kelvin.

- Liquid phase
  $c_p = 1594 + 4.33 \cdot T$
- Solid phase:
  $c_p = 1017 + 3.50 \cdot T$

An attempt of an inventory of PCM collected for $\Delta_{fus}h$ values of 264 · kJ · kg^{-1} and 226 · kJ · kg^{-1} respectively [9].

A publication of Araki et al. [10] gives values for c_p and $\Delta_{fus}h$ and states an accuracy of the measurements for both values of ± 5%. The measurements have been carried out with a twin calorimeter. Specific heat, c_p, was measured for mixtures of 60.3 wt% and 54.3 wt% of SA

respectively. The results show four linear expressions for the two concentrations and corresponding to these concentrations for the different states solid and liquid. T is in Kelvin and c_p is derived in $kJ \cdot kg^{-1} \cdot K^{-1}$.

- 60.3 wt% SA, liquid phase, 303 K ≤ T ≤ 353 K:
  $c_p = 1.56 + 4.27 \cdot 10^{-3} \cdot T$
- 60.3 wt% SA, solid phase, 303 K ≤ T ≤ 328 K:
  $c_p = 0.811 + 4.06 \cdot 10^{-3} \cdot T$
- 54.3 wt% SA, liquid phase, 303 K ≤ T ≤ 353 K:
  $c_p = 1.65 + 4.44 \cdot 10^{-3} \cdot T$
- 54.3 wt% SA, solid phase, 303 K ≤ T ≤ 328 K:
  $c_p = 1.36 + 2.58 \cdot 10^{-3} \cdot T$

$\Delta_{fus}h$ was measured for seven different concentrations of SA in a range between 47.5 wt% and 60.3 wt%. The measurements for $\Delta_{fus}h$ have been done through crystallisation of undercooled liquids at three different values of undercooling i.e. with three different starting temperatures. The temperatures at the begin and the end of each of the three measurement series with different starting temperatures were the same. The released heat during crystallisation was measured. It's stated that the results for $\Delta_{fus}h$ do not depend on the amount of undercooling and are linearly dependent on the mass concentration of SA, W(SA). W(SA) is given in wt% and $\Delta_{fus}h$ in $kJ \cdot kg^{-1}$.

- $\Delta_{fus}h = -4.62 \cdot 10^2 + 1.18 \cdot 10 \cdot W(SA)$

Measurements for $\Delta_{fus}h$ published by Wada [11] were an estimation of the value of $\Delta_{fus}h$ when the probe of SAT was mixed with roughly 10 wt% of a nucleating agent. The measurements were carried out with a differential scanning calorimeter (DSC). Prevention of evaporation during cycling was done by covering the sample (14 mg SAT) with a drop of liquid paraffin. The result for $\Delta_{fus}h$ is given with $262 \cdot J \cdot g^{-1}$.

A summary of research of interesting candidates for commercial applications in the field of PCM by 1986 includes data for SAT [12]. The heat of transition $\Delta_{fus}h$ is given with $226 \cdot kJ \cdot kg^{-1}$ and c_p for the solid salt with $2.79 \cdot kJ \cdot kg^{-1} \cdot K^{-1}$.

In Gmelins Handbook of inorganic chemistry [13] values for SAT and undercooled solutions were found [13]. c_p for the solid phase is given with $2.55 \cdot kJ \cdot kg^{-1} \cdot K^{-1}$ and for the liquid phase with $3.54 \cdot kJ \cdot kg^{-1} \cdot K^{-1}$ for SAT respectively. $\Delta_{fus}h$ is given with $161 \cdot kJ \cdot kg^{-1}$ for SAT. Table 1-1 gives values of c_p in the undercooled liquid phase for different amounts of SA in the mixture.

Table 1-1: Values of specific heat capacity, c_p, related to concentration of SA, W(SA), in the undercooled liquid. Valid for 18 °C to 20 °C. [13]

W(SA) [wt%]	$\mathbf{c_p}$ [kJ · kg^{-1} · K^{-1}]
20.5	3.70
24.3	3.62
29.8	3.52
30.9	3.50
33.3	3.45
34.4	3.45
37.1	3.41
38.6	3.36
40.2	3.32
44.4	3.26
44.8	3.24
51.85	3.090
58.42	2.943

1.4 Outline of work

The introduction of this thesis locates it in the research field of TES and tries to give a relation to its position in the context of society.
The chapter Fundamentals gives basic explanations and descriptions of applied methods and scientific background.
The third chapter is all about work carried out in the laboratory at the IWT related to this thesis. It contains experimental setup, data examination and discussion of obtained results. Descriptions of experimental setups and loops of improvement are an essential part of this work because this will help to carry out final measurements in future.
The last chapter summary and conclusions collects the gained results, relates them to problems in the project and tries to give onsets for solutions of issues described in chapter 1.2, aim of work.

2 BASICS

At the beginning of this chapter a very crucial point is to discuss the phase diagram, because it gives all the information needed to understand the behaviour of the used SA mixtures, in particular the segregation phenomenon. Triggering crystallisation is easier to understand with some theory given in the subchapter nucleation. The basis of the performed triggering experiments at the IWT is work of ancestors in the field of research of SAT and is described briefly in a subchapter. To know heat transfer rates during a storage cycle, measurements of h/T-curves have to be done. The principle of the used measuring method will be described.

2.1 Phase diagram

The investigated system SA-water shows incongruent melting which means that the crystal structure of SAT is not stable at temperatures above 58 °C and therefore decomposes.
The phase diagram in figure 2-1 is a mixture out of three different sources. The scanned copies were merged with the aid of software engauge.digitizer [14].

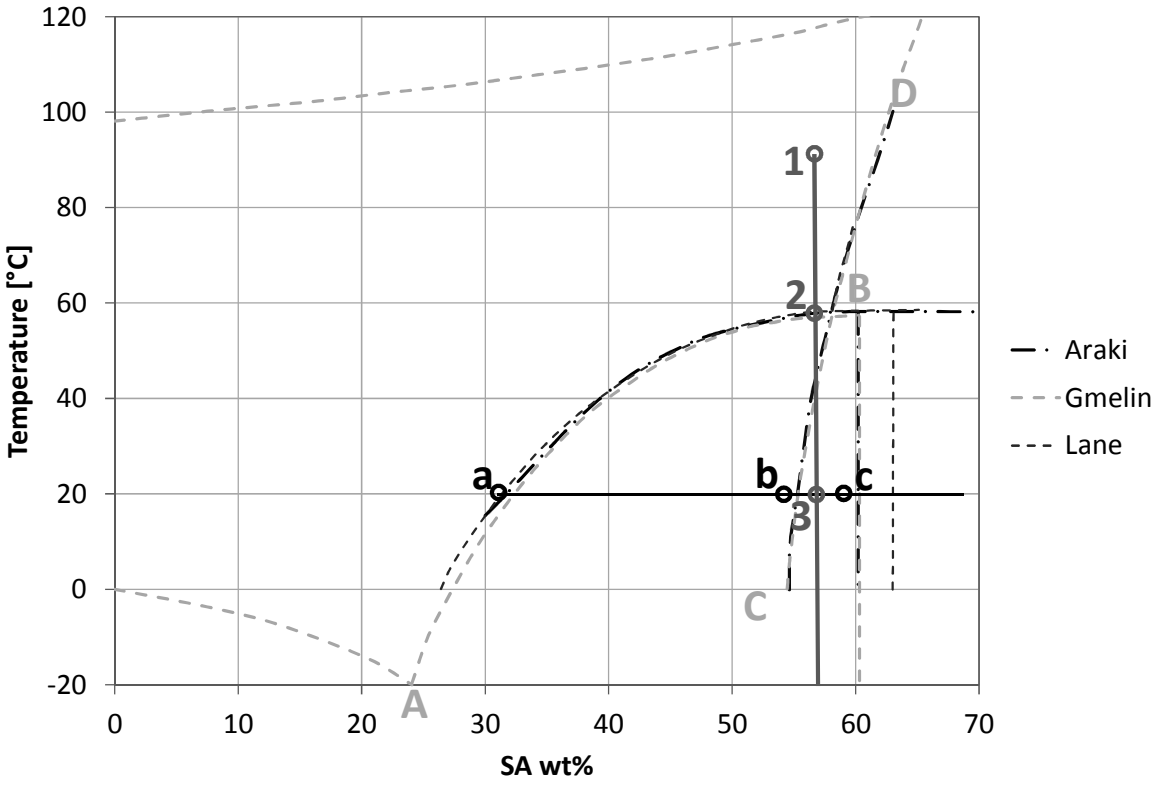

Figure 2-1: Phase diagram for the system SA water. Diagrams from three different sources are collected in this picture [15], [12], [10].

The curve C-D marks the solubility of SA in water and the curve A-B the solubility from SAT in water. Both lines are temperature dependent with increasing solubility with rising temperature. The gradient for SAT is much larger than for SA. For SAT with the mass concentration of 60.3 wt% SA the isopleth in figure 2-1 is shown as line c-B (c in lower case).

Heating SAT from 20 °C along the isopleth leads to decomposition into SA and water at point B, corresponding to 58 °C as mentioned above. At this point a solution of 58 wt% of SA in water and solid SA are in equilibrium. Thus phase change for SAT occurs at 58 °C but heating just a little above line A-B leaves solid SA in the system. Further heating dissolves SA. SA is completely dissolved at a temperature given by the intersection of the isopleth with line C-D at about 78 °C. For a solution with higher water content than SAT, e.g. 58 wt% SA, the corresponding isopleth has to be considered to get information about the melting point and solubility as undercooled liquid. Starting at point 1 of this isopleth the mixture is completely dissolved. Cooling to point 2 assuming undercooling marks the beginning of SA precipitation also known as segregation. Further cooling to point 3 additionally forms SA. Point 3 marks room temperature and the amount of precipitated SA can be found by the lever rule. The ratio of solid SA to liquid with the concentration of 55 wt% SA is about three to forty-two. It can be found, that for undercooling to room temperature without segregation the overall concentration for the mixture has to be about 54 wt% to 55 wt% SA.

2.2 Nucleation

Starting with a new subject like undercooling and triggering crystallisation, where in the beginning results of experiments are more or less unpredictable, leaves some questions concerning the theoretical background. This subchapter is intended to give an idea of the basic principles of nucleation. Except [16] and [17] literature is scarcely available.

A short historical introduction shows, that the recognition of a phenomenon like phase equilibrium dates back to somewhere in the beginning of the eighteenth century. It was thought that the freezing point of water is variable (undercooling of up to -40°C). This forced Fahrenheit and his associate to start investigations on the freezing of water. In one experiment Fahrenheit managed to undercool water to -10 °C. With his results in studying freezing of water he initiated the study of phase equilibria and of undercooling phenomena. Notable, as side effect he had to develop a serviceable thermometer which brought up the Fahrenheit scale.
The work on water of Fahrenheit was confirmed by other workers and extended to other fields of application. Interestingly the phenomena of undercooled aqueous salt solutions where discovered in 1775 by Lowitz. At the beginning of research in crystallisation, experimental results were highly inaccurate due to the intrinsic instability and the sensitiveness of undercooled conditions, where the slightest trace of a new phase or foreign material lead to crystallisation. Therefore relation of observations to parameters of state remained obscure. A thermodynamic criterion for instability, discovered by Gibbs, remained unnoticed by the time when increasingly widespread knowledge of thermodynamics and kinetics provided the background of a kinetic theory of instability. In a theory known as Volmer-Weber-Becker-Döring theory, which is a blending of thermodynamics and kinetics, the basic rules to describe the instability in those systems are put together. By the release of the used textbook (1969) a statistical mechanical theory of condensation by Meyer completes the theories of nucleation.

Easy to imagine, out of this brief glimpse on historical developments, that nucleation alone could fill a thesis. Here I state that this work is not about nucleation theory for SAT, instead this chapter should introduce in a brief way the basic background of nucleation.

In a crystallisation process it is convenient to distinguish four stages of this phase change. First it's necessary to get a supersaturated solution which may be achieved through any chemical reaction, e.g. a photoreaction, or any change of a physical property like pressure, temperature or even tension of the system. Second, the forming of the first nuclei in the new phase is needed. This may occur heterogeneously e.g. around dust particles or other surfaces or homogenously in the parent phase. Third, the growth of this particles and forth, relaxation processes which results in a altering of the texture of the newly built phase.
Interesting for this work is how to trigger crystallisation for SAT or its solutions. Triggering is related to the first and the second step of crystallisation – it is a connection of thermodynamics and kinetics which is the key to nucleation.
The basic tool to describe different states of a system like SA solutions as a function of temperature and composition is, as described in the chapter above, the phase diagram. But unfortunately the lines in this diagram are only related to thermodynamic equilibrium states of the system.

The question if a change of the system from one state to another is thermodynamically favourable (spontaneous) is answered by the difference of the Gibbs energy G of the system in these two states. Equation 2-1 shows the second law of thermodynamics in terms of the state function G. This fundamental inequality states, that if the change of G, due to a change of the system is less or equal zero, at constant temperature and pressure, the process is spontaneous.

$$\Delta G_{T=\text{const.},p=\text{const.}} \leq 0 \qquad \text{Equation: 2-1}$$

The variation of G at constant pressure with the temperature T is proportional to the entropy –S, which is stated in equation 2-2.

$$\left(\frac{\partial G}{\partial T}\right)_p = -S \qquad \text{Equation: 2-2}$$

This relationship between G and T at constant pressure is shown in figure 2-1. The proportionality to –S shows that with rising T at constant pressure, G has to decrease. Moreover, since the entropy for solids is lower than for liquids (a solid is more ordered than a liquid) the slope for solids has to be less steep than for liquids. The intersection of those two lines marks the equilibrium point of two phases of a substance at constant pressure. The quantity G has the same value for the liquid and solid phase in this point. A change form solid to liquid or vice versa would lead to a ΔG of zero at the melting temperature. Thus phase change at the melting point is a reversible process. Considering a lower Temperature like T_1 in figure 2-2 shows that at this temperature the liquid phase has a higher G than the

solid one and therefore a phase change for an undercooled liquid with temperature T_1 would be thermodynamically favourable. As known form our experiments, a SA solution with e.g. 42 · wt% of water will undercool in a stable, or more precise, metastable way, to ambient temperature and not crystallise spontaneously at its melting point of 58 · °C as thermodynamically predicted. To understand the effect of undercooling related to nucleation we have to understand what happens when a new crystal forms.

The initiation of nucleation out of clusters is thought to be a result of thermal fluctuations that built transient structures in liquids. The final formation of a stable growing nucleus out of such a cluster is dependent on its size. The relation between size and stability of a formed nucleus is subject of the classical nucleation theory for homogenous nucleation which will be outlined in the following.

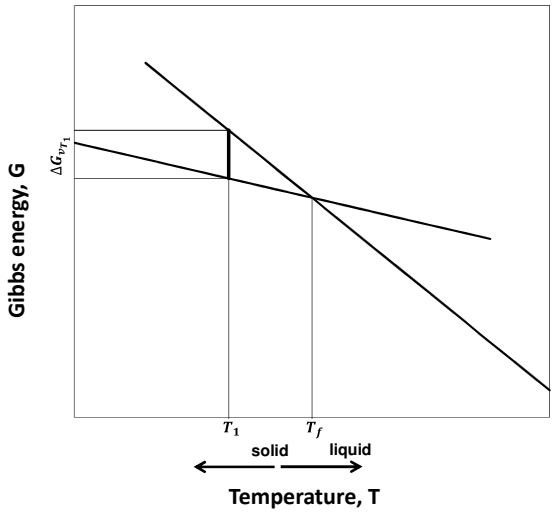

Figure 2-2: Schematic change of the Gibbs energy with temperature of the solid and liquid phase of a substance (lines are curved for real materials). The phase with the lower Gibbs energy at a specific temperature is the thermodynamicaly stable phase. At the melting point or point of fusion, T_f, the Gibbs energy for the solid and liquid are the same. T_1 is an assumed temperature of undercooling with the excess of Gibbs energy, ΔG_{vT1}, of the undercooled phase compared to the solid thermodynamical stable one.

The total change of Gibbs energy ΔG_{Ti} for building a nucleus out of an undercooled liquid is given in equation 2-3.

$$\Delta G_{T_i} = \frac{4}{3} \cdot \pi \cdot r^3 \cdot \Delta G_{v_{T_i}} + 4 \cdot \pi \cdot r^2 \cdot \sigma \qquad \text{Equation: 2-3}$$

Here ΔG_{Ti} is the sum of an “energy” delivering part of nucleation on one hand and a consumptive part on the other at a specific temperature T_i.
The first term in this equation corresponds to the energy delivering part and hence has to be negative. Here the quantity ΔG_{vTi} carries the negative algebraic sign which can be seen from 2-2. The change from the metastable undercooled liquid phase to the stable solid phase is responsible for the excess in Gibbs free energy which is the driving force for nucleation. To

make the relationship between the size of a nucleus and its stability visible, ΔG_{vTi}, is specified as volumetric value and thus has to be multiplied with the volume of the built nucleus. In the end the energy delivering term is proportional to the cube of the radius r of the nucleus and the negative quantity ΔG_{vTi}.

The second term describes the work to be done to build a new surface when a nucleus forms. It is proportional to the surface area and therefore to the second power of the radius r on one hand and to the surface tension σ on the other. It is a positive energy consuming term.

Since the positive term is proportional to r^2 and the negative to r^3 the positive grows faster with rising r in the beginning than the negative and hence there is a maximum of ΔG_{Ti}. The whole context of this problem is depicted in figure 2-3.

For T_1 the energy delivering and consuming terms are drawn apart to make the different growth of the functions visible. The sum of curves is shown for three temperatures. Restricted to the curve for temperature T_1 there is a maximum of change in Gibbs free energy at $r_{crit.,\ T1}$. This is the radius for the so called critical size of the nucleus, or critical radius. This radius represents the size of a cluster of the new phase that is in unstable equilibrium with the parent phase. Attaching more atoms from the parent phase turns the nucleus into a stable cluster and it grows whereas detachment leads to irreversible decay. This radius marks the border between a unstable and metastable size of a nucleus and is often related to the so called Ostwald-Miers-range (see also chapter 2.3) of an undercooled system. The intersection point of the sum curve with the horizontal axis marks the radius where the new built nucleus is thermodynamically stable and growth is spontaneous.

As can be seen from figure 2-2 ΔG_{vTi} has to be different for the three different temperatures of undercooling which had to be regarded for the graph of the sum curves for T_2 and T_3. The different values for ΔG_{vTi} lead to three different critical radii for the three temperatures. With rising undercooling the critical radius decreases and therefore the probability that a growing nucleus out of a transient cluster of the undercooled solution forms is rising as well.

Since the Gibbs energy of a solution like a SAT melt is not only a function of temperature but also of composition and pressure, the stability of an undercooled melt depends on those two quantities as well. In other words, triggering crystallisation can be done by control of temperature, pressure or composition.

The next subchapter is related to practical considerations on crystallisation done by protagonists in the field of research on SAT and its solutions as phase change storage material.

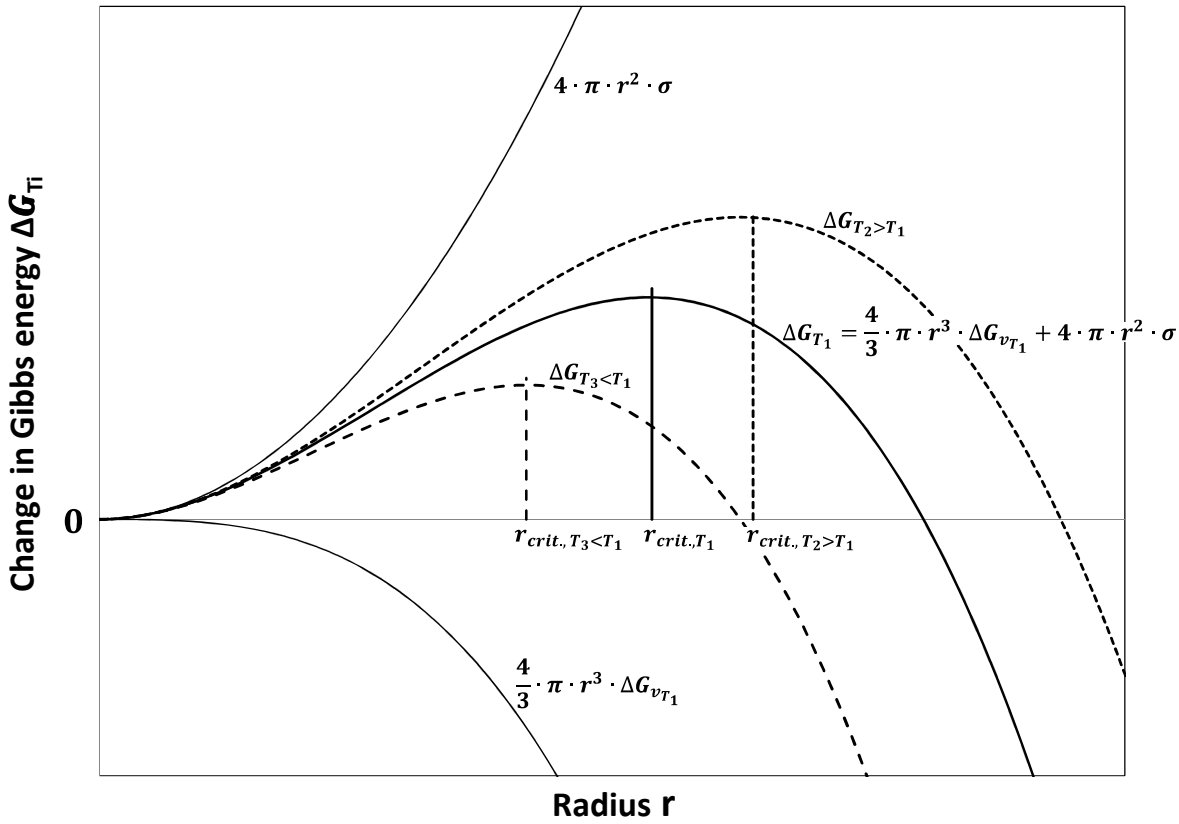

Figure 2-3 : Qualitative development of change of Gibbs energy with rising radius of a growing nucleus, built out of an undercooled melt for three termperatures T_i. The critical radius $r_{crit.}$ for spontaneous growth decreases with rising undercooling.

2.3 Triggering Crystallisation

Since undercooled SA mixtures are metastable systems it could be suggested that controlled crystallisation should be easy. It is not. This chapter should first give a summary of general aspects related to triggering crystallisation collected from literature [17].

- *Motion*
  Mechanical operations like shaking (generally known from undercooled water), scratching or rubbing could cause metastable liquids to crystallize. Out of the observation that 10^{-10} · g [note HD: how this value was derived is not explained in detail] of seed added to a undercooled liquid could cause crystallisation, it is considered that effects like scratching are likely to cause crystallisation due to attrition of crystals already present. The exertion of sound in sufficient intense of sonic radiation causes oscillation and therefore motion in the liquid which in addition could lead to nucleation.

- I*nfection and Homogenous Crystallisation*
  Stability of metastable liquid phases is related to its amount of undercooling. Spontaneous (homogeneous) nucleation occurs only in sufficiently undercooled

liquids. Two different samples which are at different states of undercooling show a different time-lag before crystallisation occurs (undercooled SAT does not crystallise instantly after reaching e.g. room temperature but within a lag of time – during segregation experiments in test tubes some samples crystallised after a few days or hours at room temperature). The often used Ostwald-Miers-range is an approach to distinguish between metastable and unstable undercooling by meanings of a distinct boundary. Unstable liquids crystallise in a short period of time while metastable phases are unchanged for an unlimited period of time. In theory undercooled parent phases should show abnormal and premonitory changes in the bulk properties on approaching the unstable state, which could be explained with the statistical mechanical theory of phase change – any investigations in this direction would have been out of the scope of this work.
Atmospheric dust and any other particles or contaminants of a sample are a source for seeds or foreign nuclei (only if they have a similar crystal structure as the probed substance) that could cause nucleation. With the explanation above about metastable and unstable phases any contaminant can lower the stability of an undercooled solution and therefore shift the boundary between stability.

- *Kinetics in Melts*
  Investigations in the kinetics of crystallisation in liquids, lead to the result, that the rate of formation of nuclei can be a function of temperature and hence is not constant after crossing the border of the metastable towards the unstable region. In other words, it is possible that the rate reaches a maximum in the unstable region e.g. observed for piperine (an organic crystalline material).

Sandnes [1] had a practical approach. He investigated different methods for triggering crystallisation in SAT. He found that in general the two basic mechanisms that lead to crystallisation are seeding and homogenous nucleation. Homogenous crystallisation is achieved by shifting the thermodynamic parameters pressure or temperature of the undercooled system (this is also the basic idea of the experiments in chapter 3.2 of this work using a Peltier element for triggering crystallisation).
A method called "cold finger" generates a local cold spot in the undercooled liquid and causes homogenous nucleation.
Triggering crystallisation with ultrasonic vibration is theoretically related to a generation of extremely high local pressure when cavities resulting from the stimuli collapse. This method was not successful for SA mixtures.
Reliable methods should be any of those like flexing of metal discs with cut slits or of coil springs. The basic principle behind these methods is the retaining of seed crystals due to high pressure in the small gaps during activation.
Methods with valve systems that separate seeding crystals from an undercooled solution of SA were not successful due to the ability of the crystal to grow through microscopic cavities.

2.4 Experimental determination of h/T-curves

A very common method to investigate enthalpy changes during variation of the temperature of a sample with unknown enthalpy temperature characteristic is a method called Differential Scanning Calorimetry (DSC). This method is quite expensive and only very small sample volumes can be used. For the SA mixtures, where effects like segregation should be investigated, small volumes will not show effects of segregation because the precipitate of SA cannot settle in the small volume. Additionally the investigation of undercooling is currently not possible due to lack of mechanism of triggering crystallisation during a DSC measurement.

A method previously applied at the IWT to investigate h/T-characteristics is based on the Temperature History Method and will be used for the measurements [1], [5]. The advantage of this method is to have sample volumes that should be big enough to observe effects like segregation.

The principle of the method is to expose a sample with unknown h/T-characteristic, here PCM, in a sample tube to a constant ambient temperature that is different from the sample temperature. This causes a heat transfer rate to or from the sample. The heat transfer rate is proportional to the driving temperature difference between sample and ambient. The proportionality can be obtained in a reference experiment with a sample of known h/t-characteristic by logging the temperature history of the sample and the ambient during measurement. Since heating and cooling will be investigated reference experiments for heating and cooling have to be carried out.

Boundary conditions for this method are that the heat transfer rate is only dependent on the measurement setup and not on the sort of sample and that the temperature of the sample and sample tube is spatial uniform during the whole experiment. Since the experiments are carried out in air as ambient the heat transfer rate is limited by convection at the outside of the sample tube. The Biot number Bi is a useful instrument to control the second condition of spatial uniform temperature. It gives the ratio of resistance to conduction in the sample to the ratio of resistance to convection on the outside of the tube, $Bi = \alpha \cdot r \cdot \lambda^{-1}$. Here r is the radius of the tube, α is the heat transfer coefficient on the outside of the tube and λ is the thermal conductivity of the sample. As long as $Bi < 0.1$ heat transfer is controlled by convection on the surface of the tube thus the sample has spatial uniform temperature. Additional to exposure to the air Bi can be reduced by thermal insulation.

3 EXPERIMENTAL SETUP AND RESULTS

The experiments carried out in this thesis can be grouped in qualitative experiments related to segregation and triggering crystallisation and experiments to investigate enthalpy temperature correlations for SA mixtures.

For all experiments it was necessary to produce SA solutions with defined concentration of water. Therefore the water content of SAT (Kemira Progusta SA3) has to be analysed. This is done by dehydrating in a drying oven (Binder FD 53, 80 °C, 48 · h) with subsequent cooling in a desiccator over silica gel. Tests with phosphorous pentoxide confirmed that most of the water was lost but not all. Weighing (analytical balance – Mettler Toledo, AB204-S) after dehydration has to be done in a quick manner because the sample absorbs water from the ambient very fast. Averaged the results of phosphorous pentoxide was only about a change in the second decimal place of achieved wt% results. Therefore dehydration to constant weight and cooling over silica gel delivers reliable results in the first decimal place of derived wt% results. In general the feedstock had a water concentration of 39.7 wt%.

Samples with defined concentration are stoichiometrically blended from SAT with known water content and de-ionised water in glass vessels of 500 ml volume. After weighing the vessels are closed with plastic screw caps and molten in the drying oven. Handling of the solution is only possible when temperature is kept above saturation because undercooled mixtures can crystallise during handling and show segregation (sample not homogenous). Transfer from storage vessels into sample and test tubes is done with an automatic pipet and a syringe respectively. Tests on actual water concentration after preparation of samples with defined concentration have not been carried out.

3.1 Segregation

As mentioned in chapter 2.1 the molten SA mixtures with a water content of less than ~ 44 wt% of water would be supersaturated at room temperature. Literature states that supersaturated solutions do not show metastable behaviour, they are unstable [15]. This means the equilibrium curve for solubility of SA in water gives the values of maximum concentration of SA at a given temperature. Therefore undercooled mixtures of 42 wt% water should show a precipitate as demonstrated in chapter 2.1. This appearance of precipitates in mixtures is generally known as segregation. Contrariwise to the states of literature it is believed that segregation for solutions of 42 wt% water is related to the filling height of a vessel. To find which of both factors, filling height and concentration, are related to segregation a simple experiment is done.

Investigations on different filling heights and concentrations of water are implemented in an experiment with test tubes. A series of test tubes filled with SA mixtures of four different concentrations and for each concentration four different filling heights was assembled. Altogether two series have been carried out where the first was done with dap water and the second series some time later with de-ionised water. The chosen concentrations for the first series are 42 wt%, 44 wt%, 46 wt% and 48 wt% of water, the heights were 2 cm, 6 cm, 10 cm and 14 cm. Out of the observations in various other experiments during my work it

was found that mixtures with 46 wt% of water did not show segregation. Therefore the concentrations for the second series with de-ionised water were adapted to concentrations of 42 wt%, 43 wt%, 44 wt% and 45 wt% of water. The filling height remained the same.
Before each experiment the new test tubes were rinsed with de-ionised water and dried in the drying oven. Transfer of mixtures from glass storage vessels was done by a syringe with long injection needles to prevent contamination of the test tube wall. The tubes were plugged immediately after filling and heated again to have completely molten start conditions.
Start of the series with tap water was June 22nd 2012, of the series with de-ionised water on October 4th 2012. The photos in the discussion were taken on October 14th 2012.

Out of three related observation with samples of 42 wt% of water another series of experiments related to segregation was arranged. The first observation was that samples containing 42 wt% of water do not melt completely during heating at about 80 °C for hours without slewing of the containing vessel. The second observation was that the amount of new built precipitate during undercooling is dependent on the amount of remaining solid before undercooling and third that the T/t-trend during undercooling contains a hold at about 40 °C (see figure 3-21 and 3-23) dependent on the amount of remaining solid.
The third and second observation shows that the amount of segregation is dependent on the concentration of SA in the molten liquid because all the undissolved precipitate at the bottom of the not shaken vessels is missing in the liquid. Furthermore it can be reasoned that having a higher concentration of SA in the mixture than the amount given by the solubility at the considered temperature of undercooling will always lead to segregation when the whole excess of SA gets dissolved. Or in other words if dissolution is not complete “unused SA” remains as precipitate. The observation of variation of holds in T/t-trends with concentration can be related to additional amounts of Δh due to enthalpy of solution.
This series of experiments should qualitatively confirm the assumed correlations between heating and undercooling of a mixture with 42 wt% of water in two different ways, once with slewing the containing vessel till complete dissolution is obtained by a clear solution and once without and therefore leaving precipitate after melting. The T/t-trends are logged during undercooling. Experiments with slewing are only done three times because it is time-consuming to get all solid dissolved but for qualitative description three experiments should suffice.

3.2 Triggering Crystallisation

Since controlled crystallisation of undercooled SA mixtures is crucial to direct the release of heat of fusion in the practical use of TES two methods to trigger crystallisation in a reproducible and controlled way were developed and tested. The mechanism of the developed Peltier unit is homogenous nucleation due to local cooling of the undercooled liquid, whereas the principle of the built mechanical device is seeding. Both methods of triggering crystallisation are introduced in the following.

Photos of the designed Peltier unit and the setup to test triggering of crystallisation in undercooled SA mixtures of 42 wt% and 44 wt% respectively are presented in figure 3-1 and 3-2. The photo on the left in figure 3-1 shows the mechanical connection of the current Peltier unit to the screw cap of the used 1000 ml glass vessel for testing the unit. Electrical cords and two encapsulated thin thermocouples are passed to the exterior of the glass vessel through a small pipe of 10 mm diameter. Sealing at the plastic cap and at the lead-through for the cords is crucial to prevent leakage of water during melting in the drying oven and to ensure stable undercooling without self-triggering of crystallisation.

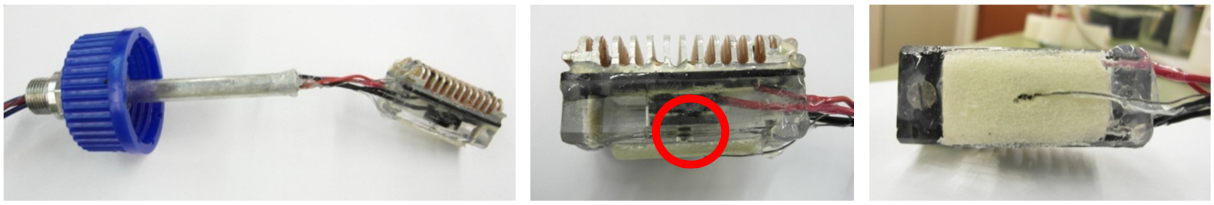

Figure 3-1: Tight assembly of Peltier-element in the cap of the bottle and detailed views of the element from the side (cavity marked with a circle) and of the "cold side".

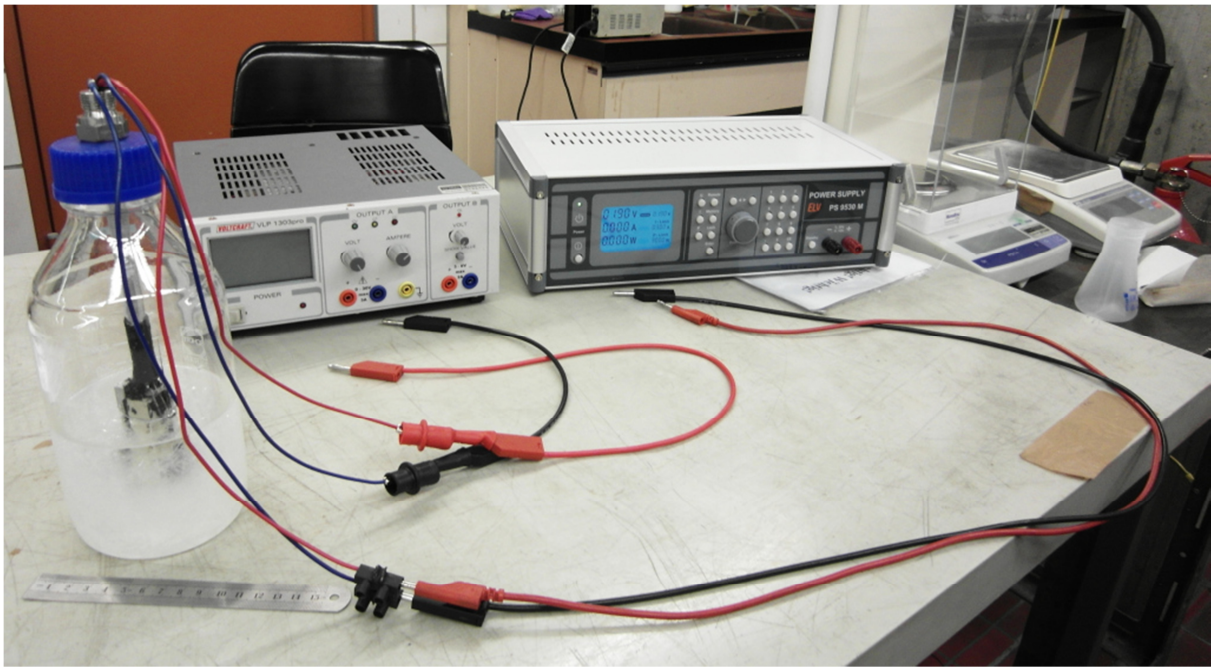

Figure 3-2: Laboratory setup for crystallisation experiments with Peltier-element in the bottle. The pictured Pelteier-unit inside the glass vessel is the first prototype but experimental setup for the final device remained the same.

The current Peltier unit is shown in the middle and on the right of figure 3-1. Main parts of the unit are a serial array of two Peltier-elements (inside of enclosure), a cooling element and an enclosure. The enclosure is built of acrylic glass for optical control of possible leaking into the unit. The two functions of the enclosure are electrical and thermal insulation of the Peltier-elements. Thermal insulation of the cold side of the unit is essential in order to use the limited heat flow rate delivered by the Peltier-elements to reach a sufficient low temperature for triggering. Only a little amount of PCM is in direct contact with the cold surface of the Peltier-element via a small cavity (marked with a circle in the middle) inside the enclosure. This

cavity is connected to the PCM on the outside via two small drills. One of the drills contains the tip of a thermocouple to detect the start temperature of nucleation. The temperature on the surface of the cooling element was controlled by a second thermocouple in order to prevent overheating of the Peltier elements.

As mentioned above experiments with SA mixtures of 42 w% and 44 wt% water were carried out. The first series of fourteen experiments was carried out with 42 wt% of water, the second series of five experiments with 44 wt%. Each experimental cycle included heating plus melting of the mixture, undercooling and finally triggering crystallisation with the Peltier device.
The experiments were the same as for the second series of segregation experiments because the thermocouple of the cooling element was able to give the T/t-curves during undercooling. From this experimental design different states of the undercooled liquid at the beginning of the triggering step in the experimental cycle were prepared. Results should give an answer wether a correlation between different dissolving conditions and the temperature of crystallisation start can be observed. A positive result would mean that the starting condition of crystallisation is dependent on the condition of dissolving. In other words, the stability of the undercooled liquid varies with boundary conditions of the experimental procedure.
Since initiation of crystallisation depends on the grade of substances the interaction of SA-solution with the containment had to be tested. Because of great thermal conductivity aluminium was the preferred construction material. But stability of aluminium drops rapidly in alkaline environment. Therefore SA samples were spiked with Al^{3+}. The effect on crystallisation was investigated.

The mechanical device was designed in first place to trigger crystallisation in the sample tubes of the planned second phase of h/T-measurements. Therefore the outer diameter of the pictured device in figure 3-3 is only 10 mm. The current mechanism is a valve that is able to bring the undercooled PCM inside of the sample tube into contact with a spot of dried SA.
In the right side picture of figure 3-3 the valve body with two axial O-rings can be seen. The opposite side of the valve body contains a radial O-ring. This is the part of the valve body that is plugged into the sample tube. One of the two axial O-rings connects the outside of the sample tube via a small drill with the undercooled PCM inside the tube. The other is a reservoir for dried SA. Completely assembled the cap (on the left of the right picture) with a PTFE plate is placed coaxial on the valve body. A spring mechanism inside the cap presses the PTFE plate against the axial O-rings and thus seals the whole tube. The cap white the PTFE plate can be twisted against the valve body. The side of the PTFE plate that is pressed against the axial O-rings contains some tiny cavities, that are able to rub some SA from the O-ring reservoir off, when twisted. During a complete rotation of the cap the cavities of the PTFE plate get in contact with both axial O-ring areas of the valve body and therefore induce crystallisation.

The design was tested with crystallisation experiments of a SA mixture with 44 wt% water. The tests were carried out with a prototype sample tube for the planned second series of h/T-measurements.

Figure 3-3: Two different views of the tiggering valve. In the right side picture the valve body with two axial O-rings is visible. One O-Ring has a small drill to connect the PTFE plate to the tube-inside and the other O-ring contains SA when completely assembled. The other part in the picture is the valve cap with the PTFE plate.

3.3 Investigation of h/T-characteristics for PCM

Experimental setup for h/T-measurements can be divided into setup for the cardboard box and setup for the sample tubes. Initial tests on the temperature distribution across the crucible chamber of the drying oven gave an unacceptable variation that should be homogenised with a cardboard box. The cardboard box shown from various positions in figure 3-7 and 3-8 consists of the outer cardboard case and the inner cardboard case (white cardboard) respectively. The four inner cardboard cases fit exactly into the outer case and divide the room of the outer case in order to have areas of defined air condition around the sample tubes. The tubes are fixed in the inner cardboard case with wire clips with a slight slope from the horizontal. Figure 3-6 shows the position of the tube in the inner case from above (left picture) and from the bottom (right picture). Air rectifying slots at the bottom of the outer case should ensure a homogenous temperature distribution. The outer cardboard case fits exactly into the chamber of the drying oven. Air flow in the case is from the bottom to the top trough the inner cases. The top of the outer cardboard case has manipulation openings for triggering crystallisation as shown in figure 3-5 on the left. The thermocouples are fixed in the outer case in a way that the sensor tips give the temperature above and below the middle of the horizontal sample tube. The complete assembled cardboard case with all the sensors in position is put into the drying oven for heating and cooling at ambient air conditions.

The sample tubes are shown in figure 3-4, disassembled on the left and completely assembled with the wire clips on the right. The steel tubes are sealed with a rubber plug at the side piece and with a rubber plug containing the temperature sensor from the opening in the right side of the pictures. In order to ensure a coaxial position of the sensor in the tube a triangular PTFE spacer is located above the upper measuring zone of the sensor as shown in the close-up on the left of figure 3-5. The whole tube is enclosed by insulation as

mentioned in chapter 2.4. The temperature sensors in the sample tubes were Pt-100 4-wire sensors class A with a diameter of 1.5 mm. The sensors for the ambient were thermocouples type K with a diameter of 0.5 mm. All sensors were calibrated together. Calibration data is collected in the appendix, table A-1. The data logger was a Solartron Group Ltd., 35951 J Universal IMP. The recording interval for all temperatures was 1 s.

With this setup the following measurements were performed:

- three runs of reference measurements with water filled tubes (ca. 8 ml water in each tube) heated in the drying oven from ambient temperature to the oven set point temperature of 70 °C and subsequently cooled at ambient.
- three runs of measurements where the tubes were filled with the investigated PCM (2 tubes with a PCM mixture of 42 wt% and 44 wt% each), heated in the drying oven to the oven set point temperature of 70 °C and subsequently cooled at ambient.
  Then crystallisation was triggered by seeding from the top of the case (see right picture in figure 3-5) and subsequently cooled at ambient again.

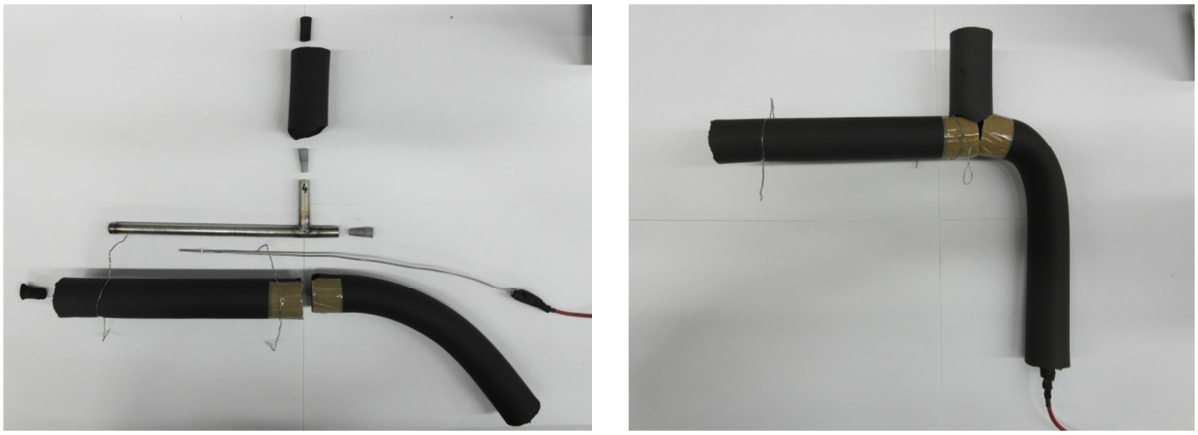

Figure 3-4: Sample tube for measurements of h/T-characteristics of PCM, first generation, made of steel. The picture on the left side shows the single components (steel tube with side piece, rubber plugs, temperature sensor, insulation and wires on the insulation for fixing the tube unit in the inner cardboard case (see figure 3-6). On the right side the assembled unit is shown.

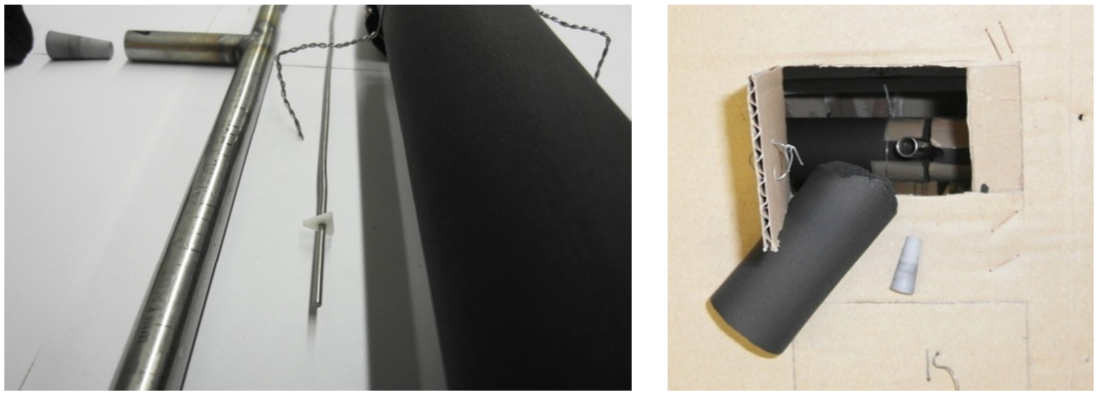

Figure 3-5: Left side picture: close-up of the temperature sensor. positioning in the tube with a spacer made of PTFE located at the upper end of the measuring zone of the sensor to ensure a centric position of the sensor in the tube.
Right side picture: access opening in the outer cardboard case for triggering crystallisation (for an overview see figure 3-8) and position of the test tube below.

Figure 3-6: Position of the sample tube in the inner cardboard case (fixed with wires) from above (left picture) and from the bottom (right picture).

Figure 3-7: Picture on the left side: outer cardboard case (seen from the back side) that exactly fits in the drying oven with cardboard guide slots to enable homogenous distribution of the heated air flow in the oven. In the picture on the right side the position of the inner cardboard case is visible.

Figure 3-8: Outer cardboard case (seen from the front side) with openings for triggering crystallisation visible on the top (left side picture). The right side picture shows the four inner cardboard cases with a samble tube assembled exemplarily in the rightmost one.

The sample tubes had some design weaknesses. Following problems were found:

- the rubber plugs were not totally tight (weight loss of ca. 0.5 % of water during the reference measurements detected); especially after the seeding it was difficult to put them into position again
- in some cases undercooling was not successful most likely because SAT crystals had fastened somewhere on the plugs and unpredictably led to crystallisation

Because of the mentioned problems a second generation of sample tubes was developed. The design of the tubes is shown in figure 3-9 (assembled) and 3-10 (disassembled). The mechanism for triggering crystallisation is positioned at the left end of the tube in the figures and described in detail in chapter 3.2.

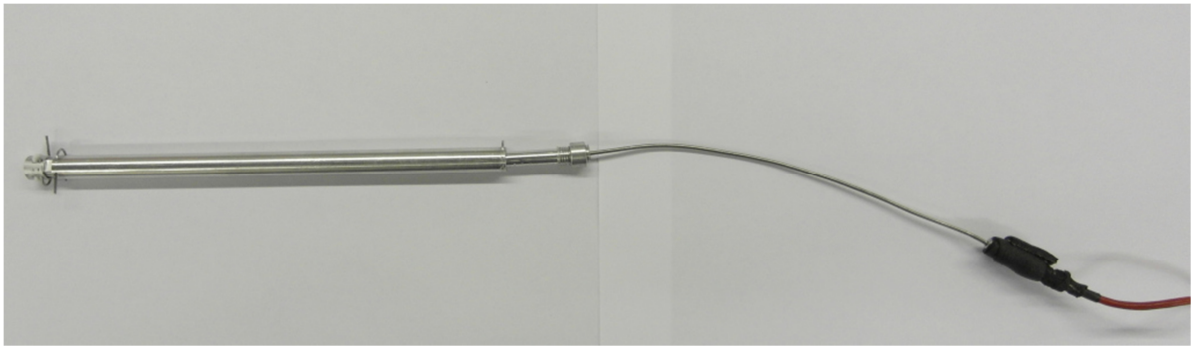

Figure 3-9: Second generation of sample tubes for measurements of h/T-characteristics of PCM made of aluminium, assembled.

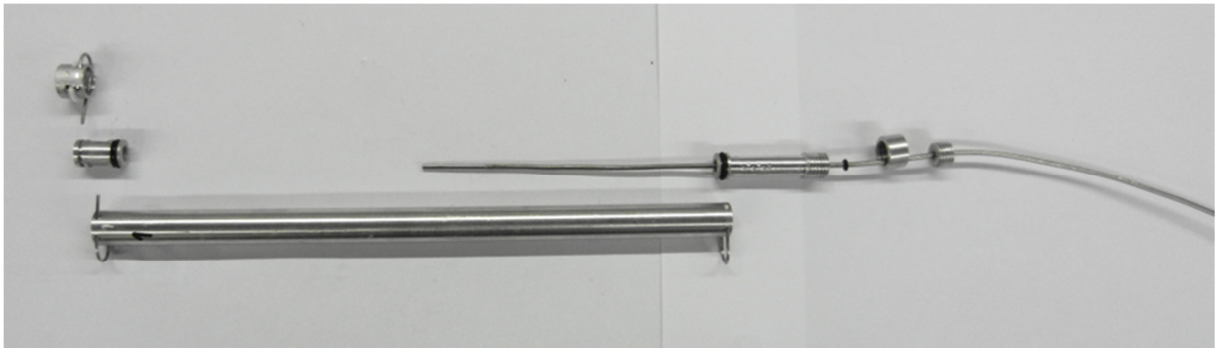

Figure 3-10: Single components of second generation sample tubes for measurements of h/T-characteristics of PCM.

3.4 Data Evaluation for h/T-characteristics of PCM

The evaluation method is in principle the same as published by Heinz in his PHD[5]. The heat exchange rate with ambient air on the sample surface by convection, $\dot{Q}_{conv}$, has to be the same like the heat storage rate, $\dot{Q}_{stor}$, of the sample, $\dot{Q} = \dot{Q}_{conv} = \dot{Q}_{stor}$. As mentioned above $\dot{Q}_{conv}$ is only a function of the temperature difference between the ambient and the sample, $\Delta T_{amb,smp} = T_{amb} - T_{smp}$ for both, the reference experiments and the experiments (using water as storage experiments) with the PCM, $\dot{Q}_{conv} = f(\Delta T_{amb,smp})$. At constant

pressure $\dot{Q}_{stor}$ of the sample equals its change in enthalpy, ΔH, divided by the considered time interval, Δt. This whole correlation is summarized in equation 3-1.

$$\dot{Q} = \dot{Q}_{conv} = f\left(\Delta T_{amb,spm}\right) = \dot{Q}_{stor} = \frac{\Delta H}{\Delta t} \qquad \text{Equation: 3-1}$$

This means for the following it would be equal to denote all heat transfer rates with $\dot{Q}$ instead of the e.g. $\dot{Q}_{conv}$ which gives only the context of the actual consideration. It is tried in the following to use the indication of the actual context. From the temperature change of the sample, ΔT_{smp}, during a reference experiment with water, ΔH can be calculated by equation 3-2.

$$\Delta H = \left(m_{H_2O} \cdot c_{p,H_2O}(T) + (m_{tube} + m_{sensor}) \cdot c_{p,steel}(T)\right) \cdot \Delta T_{smp} \qquad \text{Equation: 3-2}$$

Here m_{H2O}, m_{tube} and m_{sensor} are the mass of the water sample, of the sample tube and the temperature sensor. The material of the sample tube and the temperature sensor are both stainless steel, 1.4571. The values specific heat capacity of water, $c_{p,H2O}$, and steel, $c_{p,steel}$, are given as temperature dependent values in equations 3-3 and 3-4.
The equations are derived by fitting of data from literature [18], [20]. $c_{p,H20}$ is given in $J \cdot g^{-1} \cdot K^{-1}$ and $c_{p,steel}$ is given in $J \cdot kg^{-1} \cdot K^{-1}$ where T is in °C.

$$c_{p,H_2O}(T) = -4.749 \cdot 10^{-11} \cdot T^5 + 1.520 \cdot 10^{-8} \cdot T^4 - 1.858 \cdot 10^{-6} \cdot T^3 + 1.160 \cdot 10^{-4} \cdot T^2 - 3.492 \cdot 10^{-3} \cdot T + 4.2178 \qquad \text{Equation: 3-3}$$

$$c_{p,steel}(T) = 8.4875 \cdot 10^{-2} \cdot T + 491.61 \qquad \text{Equation: 3-4}$$

Since $\dot{Q}_{conv}$ equals $\Delta H \cdot \Delta t^{-1}$ (see equation 3-1), the relation between $\dot{Q}_{conv}$ and the corresponding value of $\Delta T_{amb,smp}$ can be derived by plotting measured values of $\Delta H \cdot \Delta t^{-1}$ from the reference experiments against corresponding values of measured $\Delta T_{amb,smp}$. Fitting of the measured points gives the relation $\dot{Q}_{conv} = f(\Delta T_{amb,smp})$.
This relation is used to obtain values of $\dot{Q}_{conv}$ from $\Delta T_{amb,smp}$ values in the experiments with PCM of unknown h/T-characteristics. It's known from equation 3-1 that $\Delta H \cdot \Delta t^{-1} = \dot{Q}_{conv}$. Therefore adaption of equations 3-2 and 3-1 to a function for Δh_{smp} gives the unknown enthalpy change, Δh_{smp}, of the investigated sample as shown in equation 3-5.

$$\Delta h_{smp} = \frac{\dot{Q}_{conv}\left(\Delta T_{amb,spm}\right) \cdot \Delta t - (m_{tube} + m_{sensor}) \cdot c_{p,steel}(T) \cdot \Delta T_{smp}}{m_{smp}} \qquad \text{Equation: 3-5}$$

The term $\dot{Q}_{conv}(\Delta T_{amb,smp})$ in this equation will be derived later on in this chapter. ΔT_{smp} is the temperature difference in the PCM sample in the considered time interval, Δt, of the measurement. The value m_{smp} is simply the mass of the investigated PCM sample.

As mentioned in the introduction, the constraint for this measurement is that the temperature within the sample is constant. This is controlled by the Biot number Bi. The calculation of Bi from experimental data from reference experiments is given in equation 3-6.

$$\mathrm{Bi} = \frac{\dot{Q}_{stor} \cdot r}{\Delta T_{amb,smp} \cdot A \cdot \lambda} \qquad \text{Equation: 3-6}$$

$\dot{Q}_{stor}$ is derived from equation 3-1and 3-2 respectively. r = 0.005 · m, is the outer radius of the sample tube. A = 7.75 · 10^{-3} ·m^2, is the outer surface of the tube (length for outer surface of tube is 24 · cm with T-piece). For examination of Bi the worst case value for thermal conductivity, λ, is used. For a SA mixture, the worst case value of λ is given for solid SAT with 0.3 · W · m^{-1} · K^{-1} [10]. For water at ambient pressure the worst value is at 0 °C with 0.56 · W · m^{-1} · K^{-1} [19]. Thus λ with 0.3 · W · m^{-1} · K^{-1} is used for the whole evaluation.

Until here basics of evaluation are discussed. In the following discussion the term for $\dot{Q}_{conv}$ ($\Delta T_{amb,smp}$) will be derived from reference measurements.

Figure 3-11 shows typical temperature/time-curves for heating and cooling of a reference measurement cycle, thus the sample tube is filled with water. The temperature of the ambient (two sensors - one below the sample tube one above the tube as mentioned above) and the sample rises when the case with the sample is put into the drying oven and fall after taking the case out again.

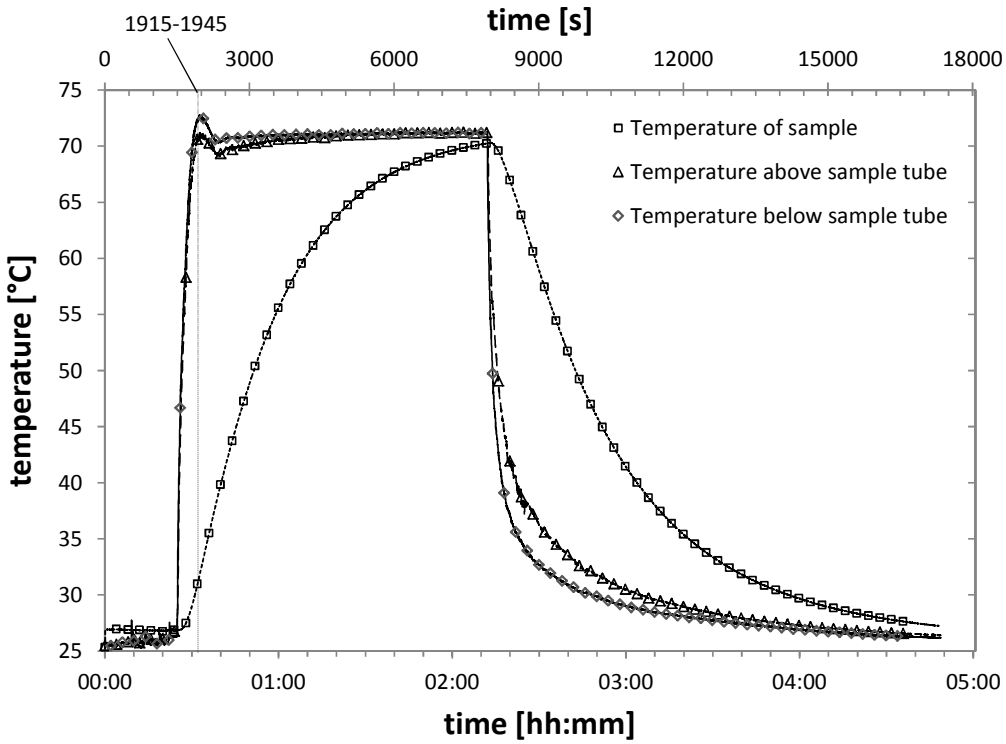

Figure 3-11: Typical temperature/time curves for heating with subsequent cooling of a measurement cycle with a water reference sample.

The data points were logged with a time interval of one second. For further evaluation data points are reduced by averaging thirty-one values for one new data point. To show that this is valid, the time interval from 1915 · s to 1945 · s is depicted in figure 3-12. This interval is marked in figure 3-11 by two dashed vertical lines as well. Seemingly one line may be registered because the interval is very narrow compared to the whole measurement interval. The chosen interval is in a range with strong curvature. If linearity is given within that interval, linear averaging is assumed to be valid for all other points and measurements as well. Since linearity is shown in figure 3-12, averaging is verified to be a correct choice (the scattering is caused by strong air movement due to the operating fan of the drying oven).
The two measured temperatures for the ambient below and above the sample are averaged to one ambient temperature T_{amb} for each time step of 31 seconds.
In general all calculations are done for the given intervals of 31 seconds. The obtained single results for each data point are either used in a diagram to derive the $\dot{Q}_{conv}$ ($\Delta T_{amb,smp}$) term or in case of the Δh_{smp} values they are summed up to h_{smp}. h_{smp} is the specific enthalpy of the investigated sample at a given temperature. The reference value $h_{smp} = 0$ is the starting point of the experiment since the temperatures are almost equal for all experiments.

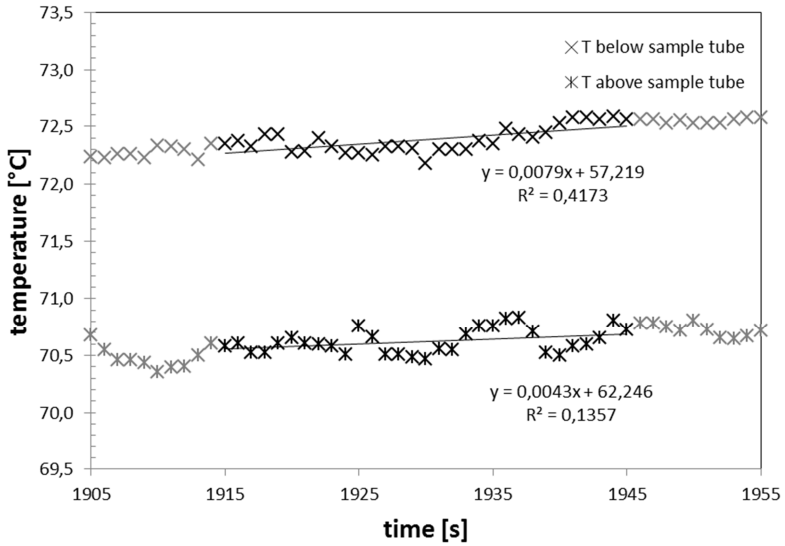

Figure 3-12: The marked time interval from figure 3-11is shown in a higher resolution to verify linearity for the chosen intervall of averaging.

Direct measured values besides temperature are the mass of the sample tube, m_{tube}, the mass of the water sample, m_{H2O} and the mass of the PCM sample, m_{smp}. The mass of the temperature sensor, m_f, is estimated by the product of its volume (length in sample tube, l = 0.115 · m, and outer diameter, d = 0.0015 · m, are measured) with the density of stainless steel (1.4571; $\rho_{1.4571}$ = 7864.5 · kg · m^{-3} [18]), $m_f = \frac{d^2 \cdot \pi}{4} \cdot l \cdot \rho_{1.4571}$. m_f is derived with 1.6 · g.

Since the data for examination of $\dot{Q}_{conv}$ ($\Delta T_{amb,smp}$) are available the calculation can be done. The correlation of $\dot{Q}_{conv}$ to $\Delta T_{amb,smp}$ for one reference measurement is depicted in figure 3-13. From hysteresis it is to assume that $\dot{Q}_{conv}$ has to be related to different steps in the whole measurement cycle. Before converting the collected data from all reference experiments to

one single term for $\dot{Q}_{conv}$ ($\Delta T_{amb,smp}$) it is needed to think about all steps of the experimental cycle in order to determine which relation for $\dot{Q}_{conv}$ will be valid for one specific time interval. There are three steps to distinguish for evaluation of the experiments with investigated PCM. The first two steps apply in principle to the reference experiments as well. The first step is heating to the melting point, melting and further heating. Second step is cooling to get an undercooled system and third step is triggering crystallisation with subsequent rise of the sample temperature, T_{smp}, to the melting point and cooling again.

- *Heating to the melting point, melting and further heating:*
  When the box is put into the oven, it heats up and T_{amb} rises. The interval of about ten minutes until constant T_{amb} is reached can be examined for a representative cycle. The comparison of the values of $\dot{Q}_{conv}$ related to rising T_{amb} with values at constant T_{amb} is given in figure 3-13 and 3-14 respectively. Figure 3-14 is time dependent while figure 3-13 is related to $\Delta T_{amb,smp}$. The correlation between the two figures is given by the marks A to G which represent the same data points in the two charts.

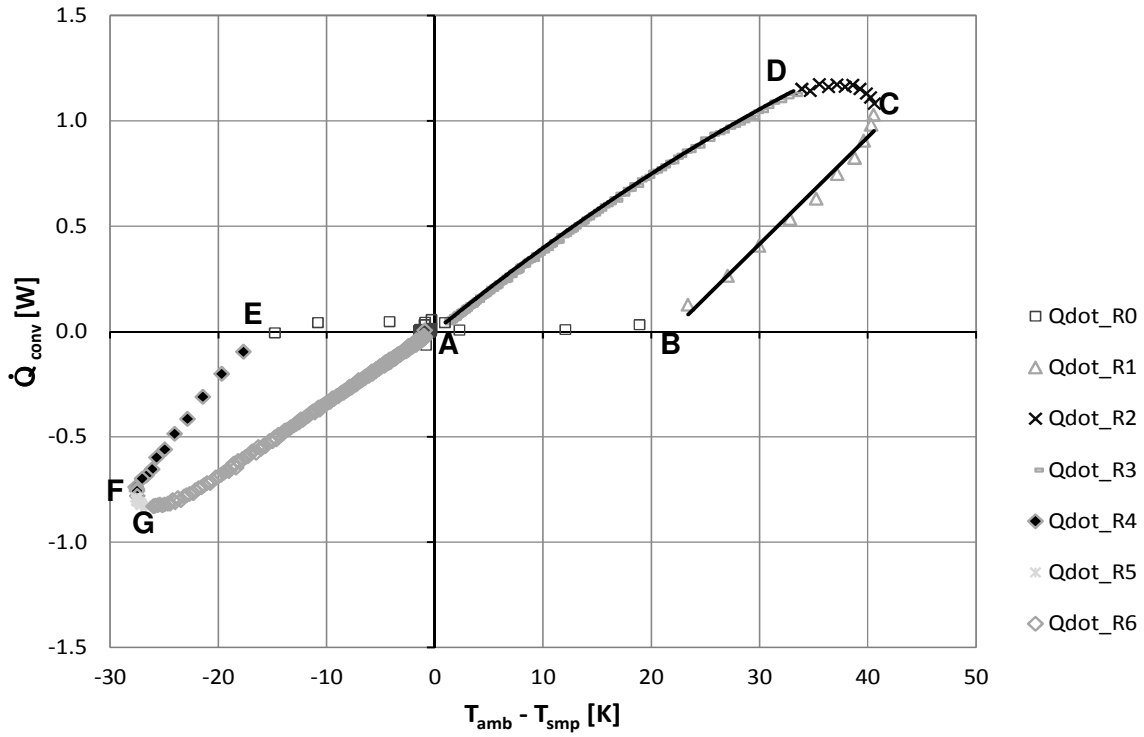

Figure 3-13: Relation between heat flow rate, $\dot{Q}$, and temperature difference of ambient and sample, $T_{amb} - T_{smp}$ for one reference measurement. The marks A to G are related to the marks in figure 3-14 and thus give the connection to the time scale during the expiriment.

Figure 3-14 gives T_{smp}, T_{amb} and $\Delta T_{amb,smp}$ varying with time. The trend of $\Delta T_{amb,smp}$ is divided into intervals by the named marks. Constant T_{amb} is reached at point D and lasts at this temperature until point A is located at the time scale. A comparison of range A to D and D to A gives the comparison of rising and constant T_{amb} mentioned

above. This is the whole interval of the heating cycle. Thus the range A-B-C-D-A is in figure 3-13 is addressed. Comparison of A-D and D-A in figure 3-13 of same values for $\Delta T_{amb,smp}$ gives different values of $\dot{Q}_{conv}$. The decision to start evaluation after constant T_{amb} would lead to a gap of ten minutes where for more than five minutes a heat transfer rate of about $1 \cdot W$ would not be registerd as exchanged heat (compare figure 3-14). This would lead to a failure of more than $300 \cdot J$ while the heat energy exchange of the whole experiment accounts for round about $4000 \cdot J$. Therefor for further evaluation the heating cycle has to be divided into intervals. The chosen intervals are given in principle in figure 3-13 with the letters A to D. For the first interval, A-B, it is assumed that $\dot{Q}_{conv}$ is always zero, for B-C and D-A fitting curves (denoted in figure 3-13) are gained from all collected reference experiments. Data points in the range of C-D are treated with constant values for $\dot{Q}_{conv}$ from the average of the last value of B-C and the first of C-D for investigation of PCM. For reference experiments the interval C-D is skipped.

The criteria to determine the marked boundaries A to G are different for the measurements with reference and investigated PCM samples respectively.

For the reference measurements the criteria are as follows. The criterion to determine the interval A-B is the difference between $\dot{Q}_{conv,i}$ and $\dot{Q}_{conv,i-1}$, $\Delta \dot{Q}_{conv}$, where the subscript i marks the considered value of the time step i and i-1 the value from the time step before. All values before the interval where $\Delta \dot{Q}_{conv}$ is continuously greater than zero are assigned to the interval A-B and therefore skipped. The criterion for point C was the difference in $\Delta T_{amb,smp}$ between two time steps. For $\Delta\Delta T_{amb,smp}$ (the change of $\Delta T_{amb,smp}$ in a time step Δt) continuously below zero between a time step i and i-1 the value belongs to the interval C-D. The limit at point D is derived from the graphical second derivation of $\dot{Q}_{conv}$ ($\Delta T_{amb,smp}$) ≈ 0. Skipping of values at the limit D of interval C-D has been done manually.

The criteria for the measurements with investigated PCM samples are related to the derived terms for $\dot{Q}_{conv}$ ($\Delta T_{amb,smp}$). The given values in the following are the starting and end points of the fitted curves. The criterion in the interval B-C is for point B $\Delta T_{amb,smp} \geq 20 \cdot K$ and for point C the same as for the reference experiments. Interval A-B is given automatically by border B discussed before and the start of the experiment. Point D is determined with $\Delta T_{amb,smp} \leq 33.6 \cdot K$ for the interval D-A. The end of intervall D-A is given with $\Delta T_{amb,smp} < 0 \cdot K$.

- *Cooling to ambient to get an undercooled liquid:*

  This step of the cycle is the reverse of the heating cycle. The relevant intervals in figures 3-14 and 3-13 for rising T_{amb} are A-E, E-F and F-G and the interval for constant temperature is G-A. The treatment is the same as for cooling. Values of $\dot{Q}_{conv}$ are assumed to be zero for the range A-E, fitting is applied for E-F and G-A and the constant average from the last value of E-F and the first of G-A is used for F-G. The determination of limits is basically the same as for the heating interval but

adapted logically for both, the reference experiments and the experiments with investigated PCM.

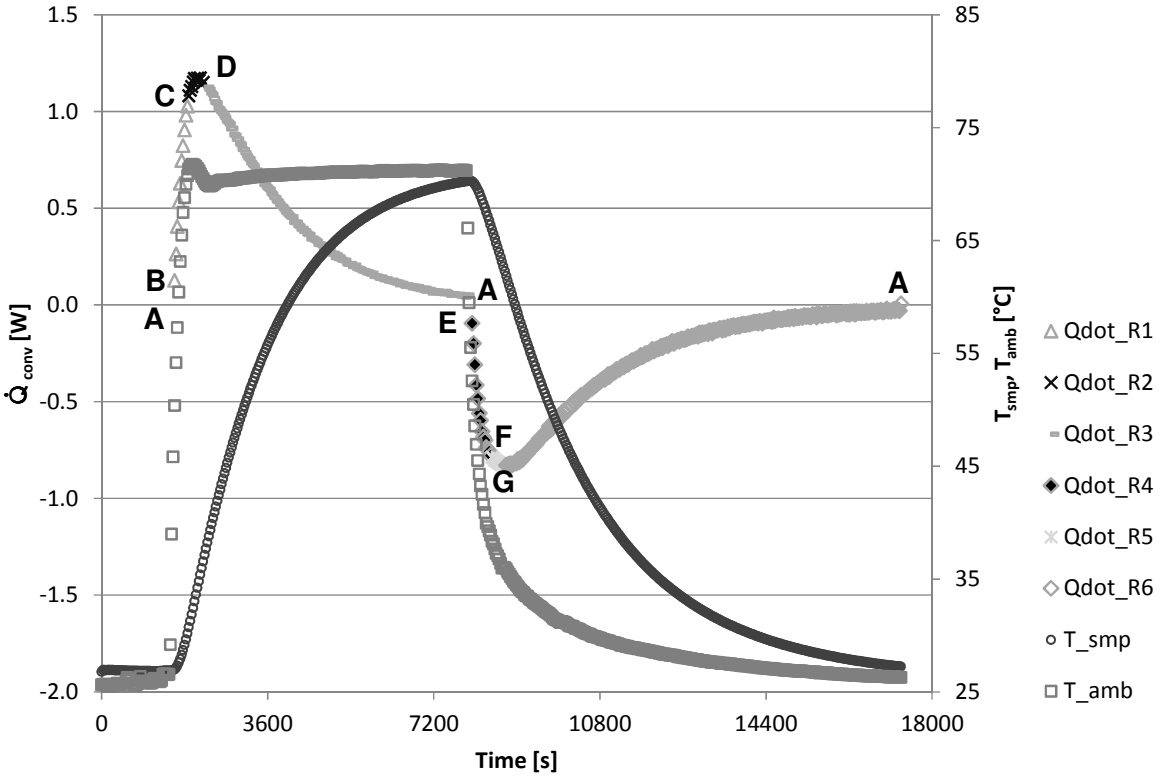

Figure 3-14: This figure relates heat transfer rates, $\dot{Q}_{conv}$, to the trend of measured temperatures of sample, T_smp, and ambient, T_amb, during a reference heating and cooling cycle. The marks A to G give the relation to equal data points in figure 3-13.

- *Triggering crystallisation with subsequent rise of T_{smp} to the melting temperature and cooling again:*

  This step of the cycle is different from the previous steps. T_{amb} is almost constant during the whole cycle which means no special treatment has to be done relating the heat transfer rates because of varying T_{amb}.

  The point to consider here is that immediately after crystallisation the temperature of the sample and the tube is not uniform. As can be seen in figure 3-15, the heat of phase change brings the sample to the melting temperature within ten to fifteen seconds but in the first minutes the temperature drops very fast and then changes over to a normal cooling curve. It can be assumed that the steel tubes are still cold when the temperature sensor records the melting temperature. The sudden drop in temperature afterwards can be explained with the sensible heat used to bring the temperature of the steel tube to the temperature of the sample. If this sample temperatures would be used to calculate $\Delta T_{amb,smp}$, the gained heat transfer rates in this time interval would be too high. On the other hand, the thermal mass of insulation is not considered in the general evaluation method. With the experimental setup it is

not possible to quantify the amount of energy that is used to heat this thermal mass. Therefore the evaluation is done with the fit of the range G-A in figure 3-13.

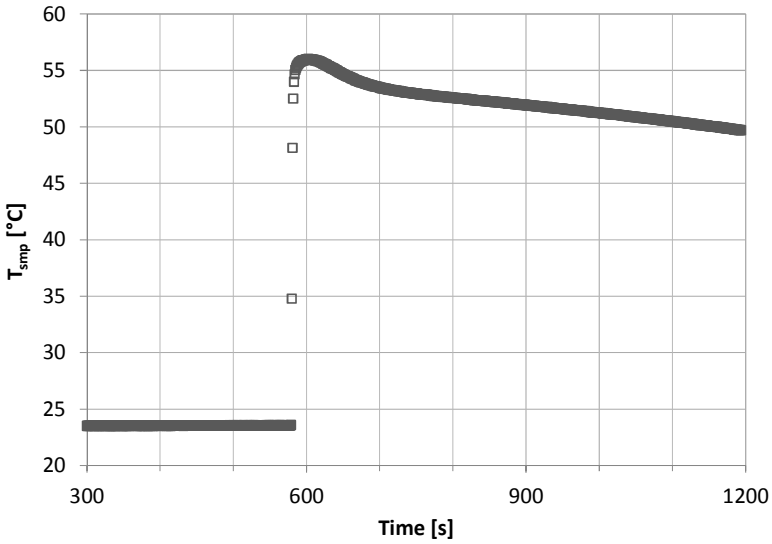

Figure 3-15: Thermal inertia of a PCM sample after start of crystallisation. Temperature rises in 10 · s after crystallisation to the melting point with subsequent temperature decrease within the first two minutes due to the thermal mass of the steel sample tube.

Finally all reference experiments are converted to $\dot{Q}_{conv} = \Delta H\, \Delta t^{-1}$ and $\Delta T_{amb,smp}$ values in order to derive the $\dot{Q}_{conv}$ ($\Delta T_{amb,smp}$) terms for the different intervals mentioned. Figure 3-16 gives an overview of all values for $\dot{Q}_{conv} = \Delta H\, \Delta t^{-1}$ and $\Delta T_{amb,smp}$.

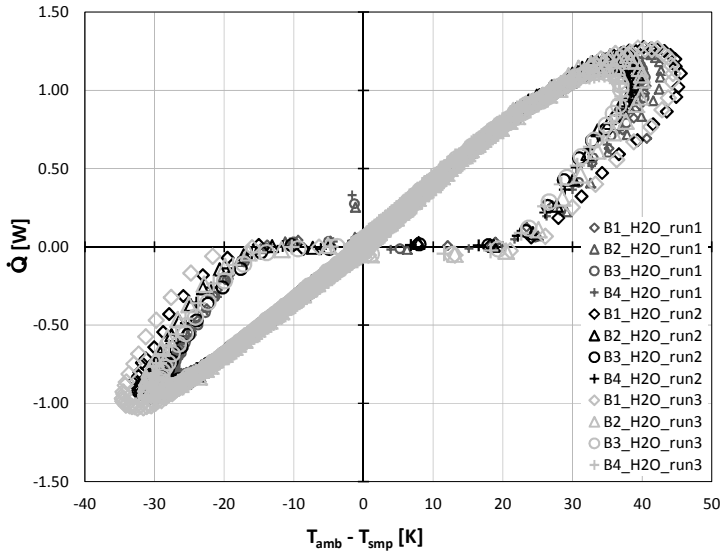

Figure 3-16: Corresponding data for $\dot{Q}$ and $T_{amb} - T_{smp}$ are given in this chart. Strong scattering in the right lower and left upper areas of the trend is related to the initial phase of heating and cooling respectively.

No correlation neither between three different measurements with one sample nor between the four samples in one measurement has been obtained. Therefore all collected values from the three measurements were used to get the four $\dot{Q}_{conv}$ ($\Delta T_{amb,smp}$) terms. The used data

points to derive fits for the intervals named above and the received terms are depicted in figures 3-17 and 3-18. According to the discussion about evaluation intervals above and according to the marks in figure 3-13, values between A-B, C-D, A-E and F-G were skipped which can be seen by comparison of figures 3-16 to 3-18.

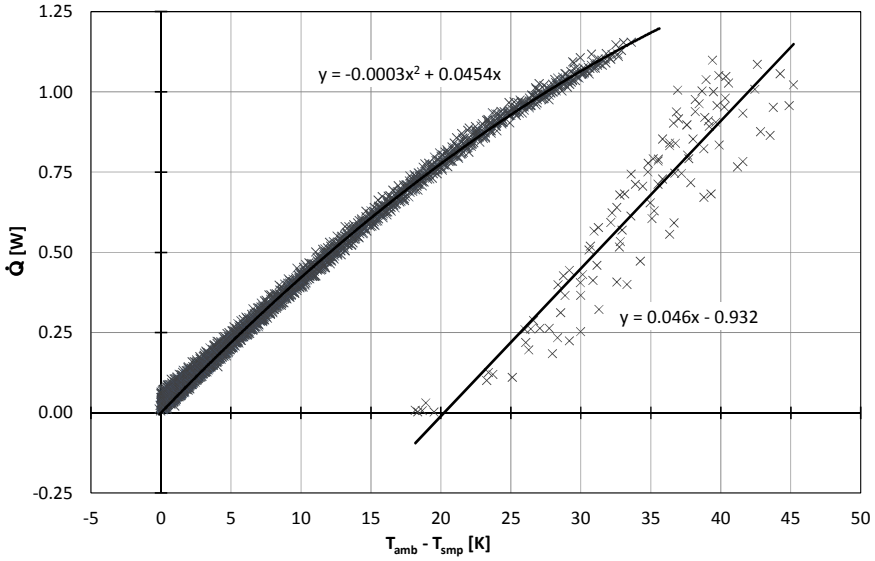

Figure 3-17: Experimentally obtained trend of $\dot{Q}_{conv}$ ($\Delta T_{amb,smp}$) from all reference experiments for the heating step. Fitting curves correspond to the marked areas B-C and A-D in figure 3-13 for the heating step of the experimental cycle.

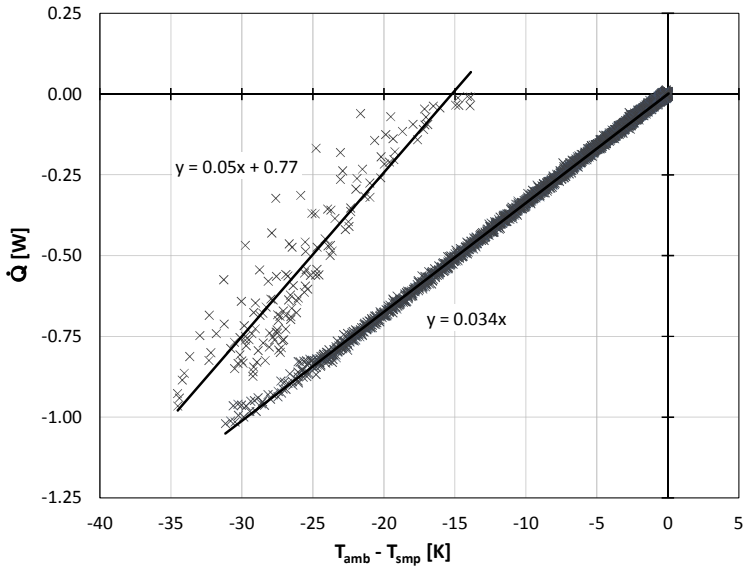

Figure 3-18: Experimentally obtained trend of $\dot{Q}_{conv}$ ($\Delta T_{amb,smp}$) from all reference experiments for the cooling step. Fitting curves correspond to the marked areas E-F and G-A in figure 3-13 for the cooling step of the experimental cycle.

Now complete evaluation can be done with the measurement data. The original data are collected in the appendix. Table 3-1 gives an overview of the data format of the collected temperature measurements. Temperatures were logged with a time interval of one second as mentioned above. The collection of experimental temperature data is carried out in charts

with trends of temperature evolution during the measurements. Three reference measurements with water and three measurements with PCM have been carried out. A table with weight of samples and sample tubes for T-History measurements is given in the appendix as well.

Table 3-1: Overview of data format for one reference measurement to determine heat transfer rates $\dot{Q}_{conv}$ of four sample tubes. Collected data are the time and the temperatures of the four samples (B1 to B 4) and of eight ambient temperatures (TC1 to TC8). Even numbers of TC_i refer to temperatures measured below the sample tubes odd numbers to temperatures above the tube. Relation between B_i and TCi is in ascending order, thus B1 is related to TC1 and TC2 and so on. Time interval for data logging is 1 · s.

		B1	B2	B3	B4	TC1	TC2	TC3	TC4	TC5	TC6	TC7	TC8
		[°C]	[°C]	[°C]	[°C]	[°C]	[°C]	[°C]	[°C]	[°C]	[°C]	[°C]	[°C]
11.07.2012	14:42:54.000	25.302	25.461	25.571	25.541	25.478	25.196	25.360	25.194	25.483	25.291	25.414	25.248
11.07.2012	14:42:55.000	25.317	25.478	25.571	25.541	25.454	25.196	25.373	25.170	25.483	25.304	25.414	25.273
11.07.2012	14:42:56.000	25.320	25.478	25.576	25.557	25.479	25.184	25.349	25.134	25.483	25.304	25.415	25.261
11.07.2012	14:42:57.000	26.934	26.760	27.014	27.253	25.691	25.638	25.634	25.613	25.679	25.597	25.756	25.639
11.07.2012	14:42:58.000	26.917	26.741	26.996	27.252	25.728	25.651	25.659	25.601	25.704	25.597	25.756	25.615
⋮	⋮	⋮	⋮	⋮	⋮	⋮	⋮	⋮	⋮	⋮	⋮	⋮	⋮
11.07.2012	19:31:48.000	27.221	27.269	27.298	27.475	26.400	26.166	26.464	26.080	26.584	26.079	26.589	26.266

3.5 Discussion of measurements results

In this section the observations and results from the experiments carried out in terms of the three main issues evaluated in this work - segregation, crystallisation and h/T-characteristic - are presented and discussed.

3.5.1 Segregation

Results of segregation experiments with test tubes are shown in figure 3-19 for the series with tap water and in figure 3-20 for de-ionised water. Each photo in the figures represents one concentration of SA and the order of photos is with ascending concentration from left to right. The filling height in each picture rises from left to right.

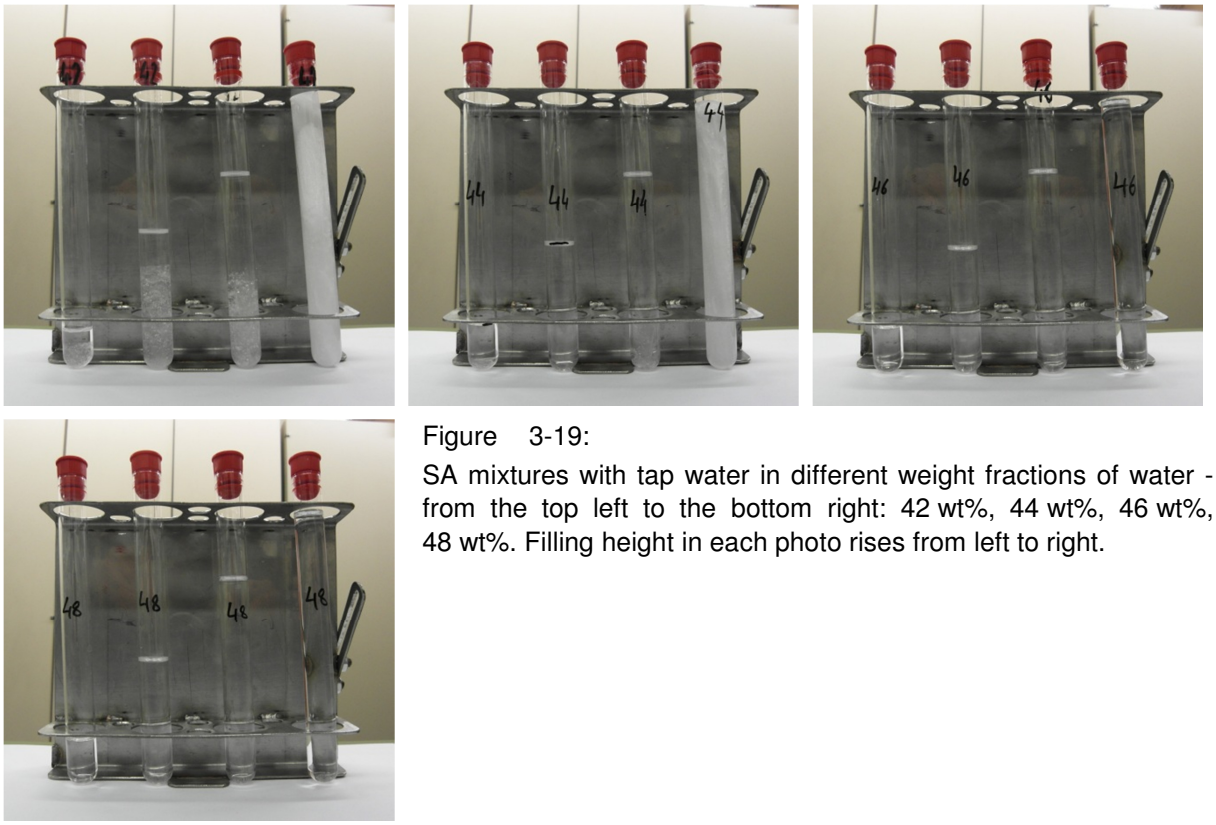

Figure 3-19:
SA mixtures with tap water in different weight fractions of water - from the top left to the bottom right: 42 wt%, 44 wt%, 46 wt%, 48 wt%. Filling height in each photo rises from left to right.

It can be seen that two of the samples in figure 3-19 crystallised. This is a result of the effect that SA solutions show strong leakage which often results in subsequent crystallisation.
In both experiments all sample tubes with 42 wt% of water show segregation whereas the height of precipitate seems not to be related to the filling height of the sample tube. Samples with 43 wt% of water in figure 3-13 show segregation for all except one sample tube but not in the tube with highest filling height. Some samples for concentrations of 44 wt% show segregation but none of the tubes with higher concentrations of water. Summarizing it can be stated that segregation is not directly related to filling height but strongly related to concentration. Concentrations above 44 wt% do not show segregation.

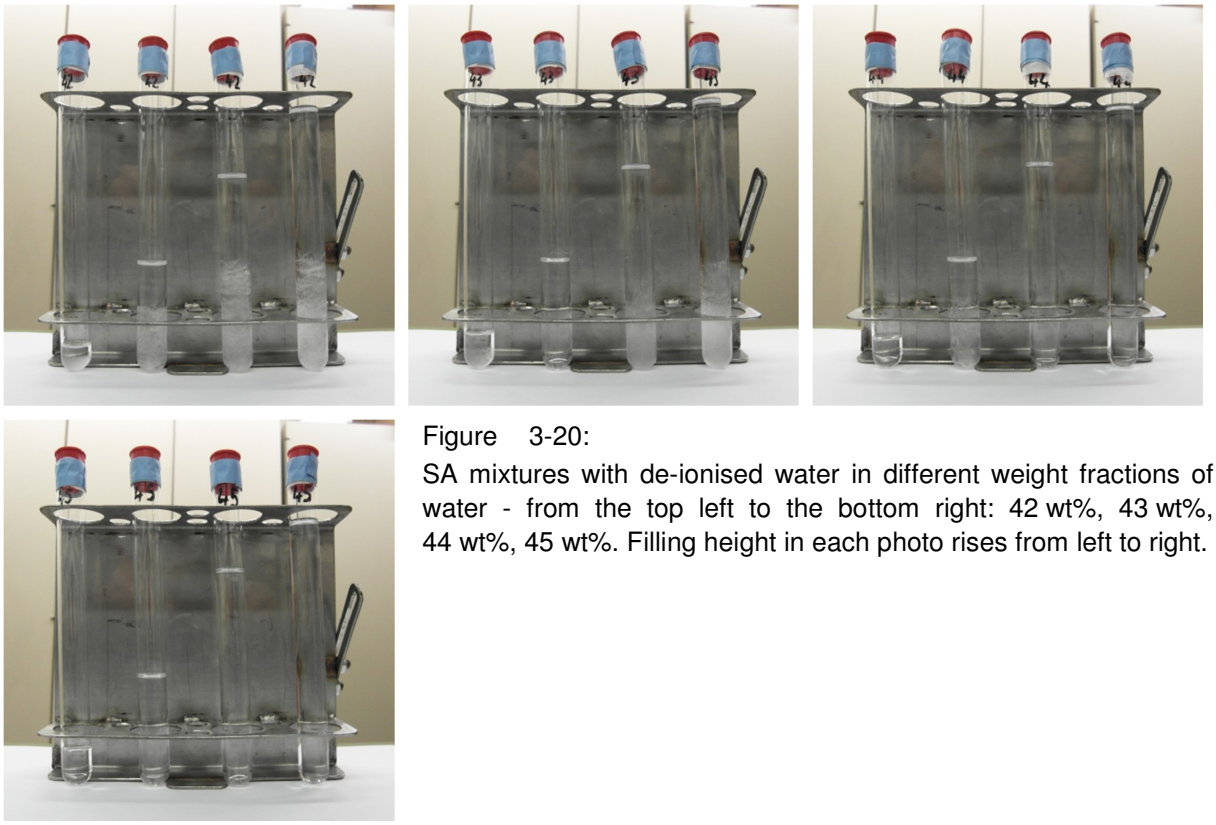

Figure 3-20:
SA mixtures with de-ionised water in different weight fractions of water - from the top left to the bottom right: 42 wt%, 43 wt%, 44 wt%, 45 wt%. Filling height in each photo rises from left to right.

The second series of segregation experiments show the assumed correlations between precipitate and holds in the T/t-curves. Figure 3-14 shows a typical hold at about 43 °C in the T/t-trend during undercooling. The appearance of this slope could be correlated to the appearance of the white precipitation, shown in figure 3-15, by taking photos in an interval of five minutes during undercooling from 80 °C to room temperature over several hours in ambient air. T/t-courses for other runs of these experiments are shown in figure 3-16. These samples undercooled much faster because they were cooled in a water filled reservoir. The curves cool_08, cool_09 and cool_10 had precipitate between 1 cm and 2 cm, curves cool_11, cool_12 and cool_13 were completely dissolved when put out of the oven for undercooling. The holdings appear for the completely dissolved samples as predicted and did not appear for the others. Figure 3-24 gives an example for the undissolved precipitate in experiments without slewing. The left of the two photos was taken earlier than the right one and shows a pile of precipitate that was dissolved later on. The photo on the right shows the undissolved precipitate after heating without slewing for hours.
It can be assumed that due to stratification in the vessel, saturated solutions at the bottom appear. Slewing attenuates this saturated layer and some precipitate gets dissolved. Thus slewing leads to complete dissolution when repeated often enough. This assumption is additionally supported by the observation of cords at the bottom of the vessel at the beginning of slewing. The effect that dissolution of samples with 42 wt% of water is difficult without convection was observed from Fan et al. as well [8].

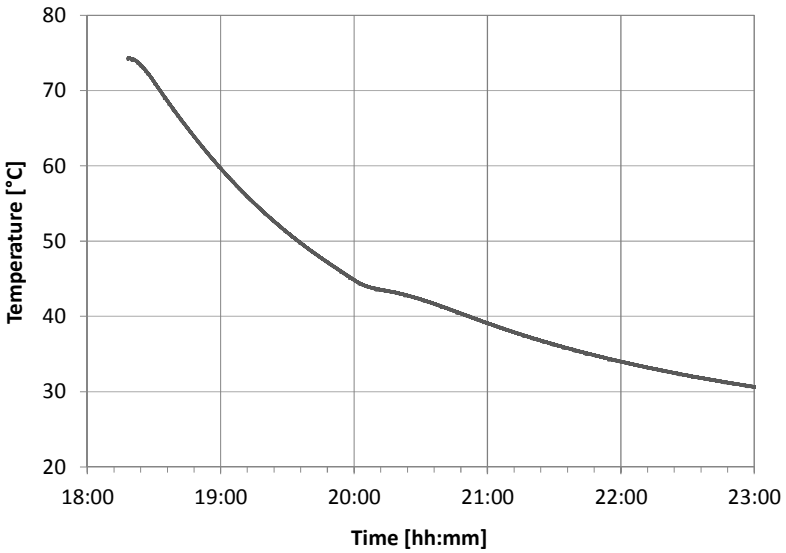

Figure 3-21: This chart shows a typicl hold in a T/t-curve during undercooling of SA mixture of 42 wt% of water after complete dissolution. For cooling the bottle was exposed to ambient air in order to take photos of the appearence of precipitate. The observed hold can be related to the photos in figure 3-15 by the given time marker.

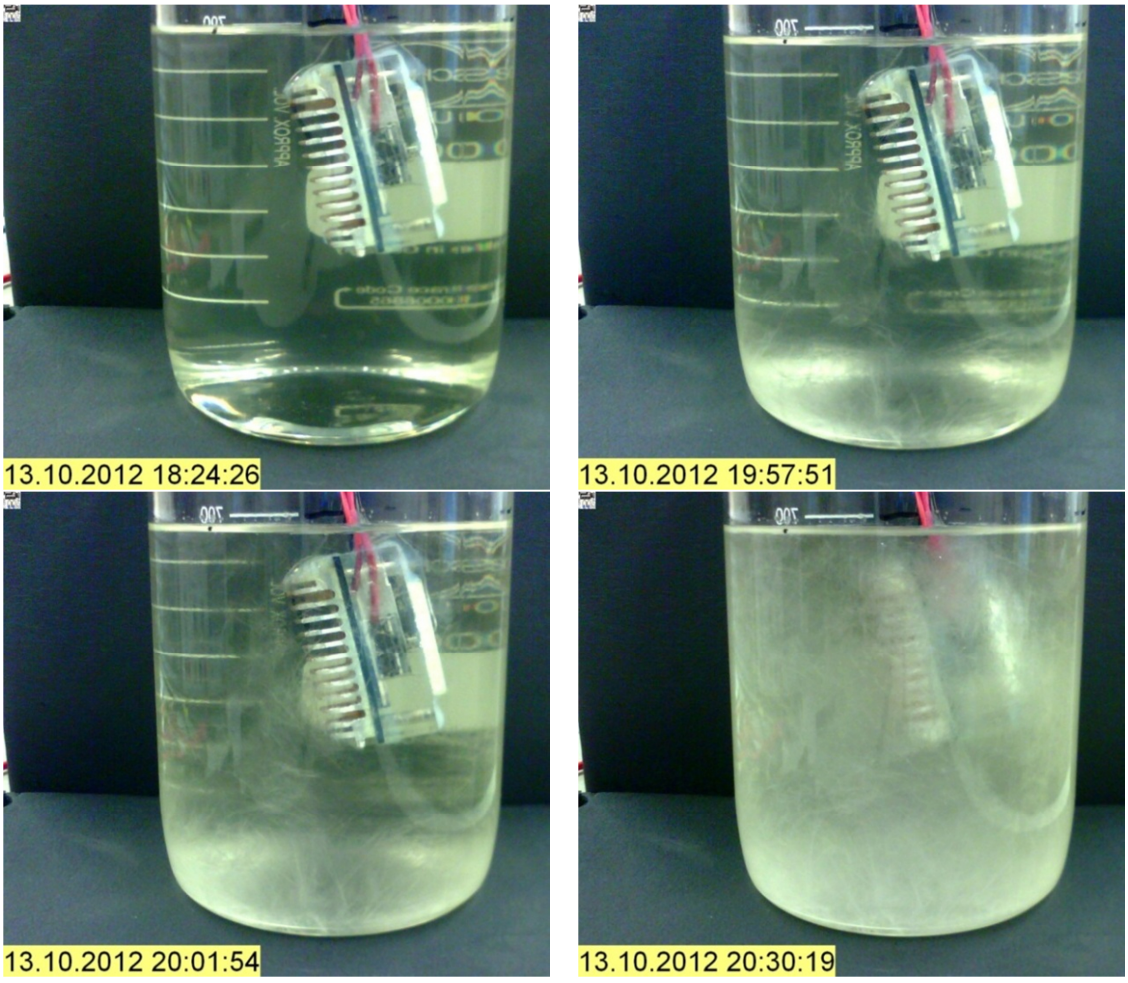

Figure 3-22: These photos were taken to show a correlation to the hold in the T/t-curve in figure 3-14. The initial state of undercooling is given in the top left and three consecutive photos of the building of precipitate follow. A relation between the tow figures is given by the time stamp.

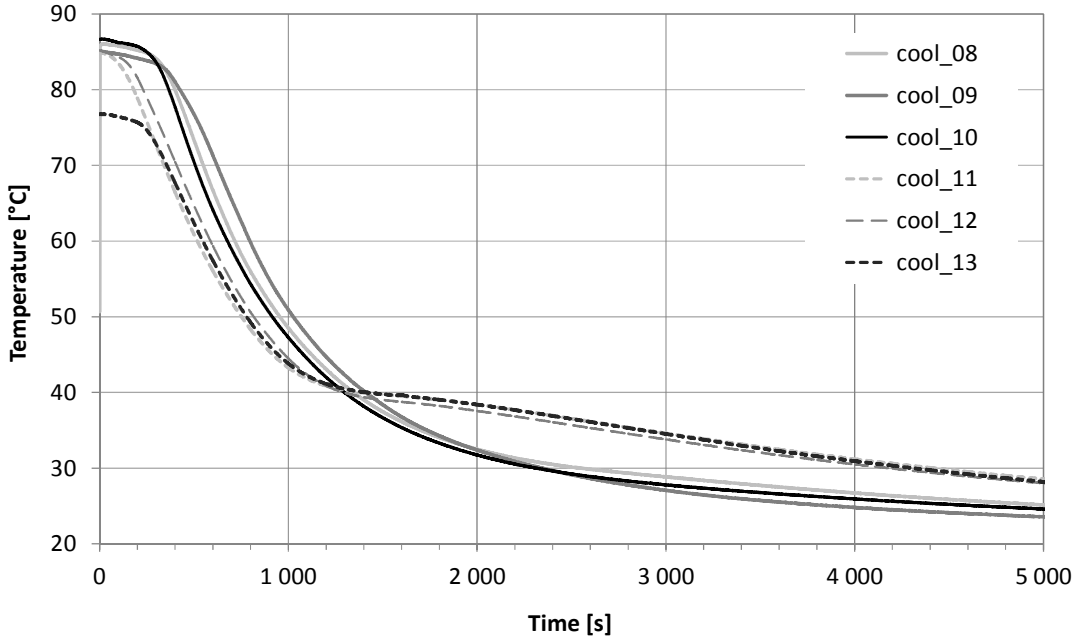

Figure 3-23: Cooling of a SA mixture with 42 wt% of water in a water filled reservoir. The curves cool_08, cool_09 and cool_10 had precipitate between ca. 1 and 2 cm when taken out of the drying oven. Curves cool_11, cool_12 and cool_13 show a hold at ca. 40 °C in the diagram, the fluid in the bottle was totally clear when taken out of the drying oven.

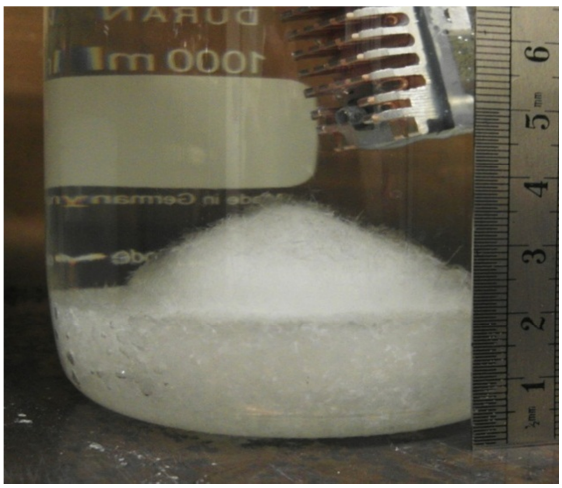

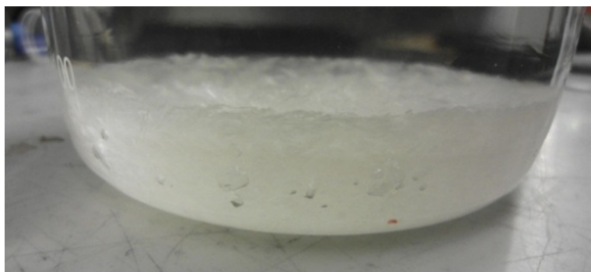

Figure 3-24:
The left photo shows the same sample of a SA mixture with 42 wt% water as in the right. It was taken before the pile in the middle dissolved. The rest of the precipitate in the right did not dissolve without slewing.

3.5.2 Triggering crystallisation

The results of triggering experiments will be presented in this chapter. Since findings in experiments with the mechanical device show unexpected behaviour that applies to experiments with the Peltier units as well they are discussed first, followed by a series of break-trough results of the experiments with the Peltier unit.

The exact number of experiments carried out with the mechanical triggering device cannot be mentioned due to improvement of the valve mechanism along the series of experiments and therefore slightly different experimental setup but about thirty successful triggered crystallisation experiments were made.

A general observation during the experiments was that during melting in the drying oven inside the tube the pressure increased. Since it was only little pressure difference it was ignored. A second observation was very little weight loss of the sample tube during the experimental series. The observed weight loss was less than in the h/T-measurements with steel tubes therefore it was assumed that the sealing with O-rings is not completely tight and some water evaporated. When first tests of the second series of h/T-measurement was launched the newly built sample tubes (same design as the prototype used in this triggering experiments) showed extremely high pressure increase when heated with water.
Since the sample tube material was aluminium the assumption that reaction with water causes the pressure came up. The decision to use aluminium was because it is easy to machine in the workshop and literature states that no corrosion effects with SA mixtures should emerge [21], seemingly by ignoring the amphoteric character of aluminium and the pH-dependent stability . Tests in advance on weight change with a piece of the later aluminium bodies in a SA mixture of 42 wt% water over several days at 80 °C did not show any changes in weight. Asking the textbook [21] gives following ideas:
Aluminium is stable against corrosion in air due to its passivating oxide-film on the surface although its reactivity with oxygen is very high (flashlight for photography in former times). Anodic oxidation is a technical process in which aluminium gets a controlled layer of anodised coating which is very resistant against corrosion in a wide area of work environments like weather, seawater, acids and alkaline lye. In the performed experiments with water this film seemed not to be built in a sufficient manner because the oxide film was only generated by natural oxidation after mechanical processing. This could be the reason for high pressure in the test-tube due to hydrogen evolution because of oxidation like in the following explanation of possible reactions:
Aluminium should not be attacked by water at room temperature because of the low solubility of aluminium hydroxide (K_L = $c(Al^{3+})$ * $c(OH^-)^3$ = $1.9*10^{-33}$ * mol^4*l^{-4}) and therefore a passivating film of aluminium hydroxide should be built on the surface of the aluminium tube.
The amphoteric character of $Al(OH)_3$ causes dissolution in alkalescent solutions ($Al(OH)_3 + H_2O \rightarrow Al(OH)_4^-$). Solutions like sodium acetate solutions are alkalescent which causes dissolution of the passivating $Al(OH)_3$-film. As result of the missing film aluminium will be oxidized under formation of H_2 at the same time ($Al + 3\ H_2O \rightarrow Al(OH)_3 + 1.5\ H_2$). The reaction will proceed until the chemical equilibrium is reached either through the pressure of H_2 or the concentration of $Al(OH)_3$.

Summarizing it can be assumed that pressure inside the tube after heating arises due to H_2 formation. The difference in height of pressure between samples with water and samples with a SA mixture can be explained assuming that the precipitate of $Al(OH)_3$ in the tubes with water does not form a closed film and therefore equilibrium is not reached. The lower pressure in the tube with a SA mixture could be explained with the fact that this tube was not machined at the inner surface or the formation of a coating layer. To find out if the assumptions are correct further experiments have to be done in future.

Triggering experiments with the Peltier device were successful for all runs. Figure 3-25 shows the first seconds of crystal growth after triggering in a time step of roughly 2 s. The first picture shows the Peltier device before homogenous nucleation sets in. The circle marks the area of the cavity in the picture.

Temperatures were homogenous nucleation begins vary in a wide range. For experiments with a SA mixture of 42 wt% of water in a range of -16 °C to -2 °C, for 44 wt% of water in a range of -15 °C to +1 °C. Since after the first three measurements with 42 wt% of water the temperature for homogenous nucleation jumped from first roughly -16 °C to -8 °C it was assumed that probably aluminium from the cooling element got dissolved and changed stability of the undercooled liquid. To find out wether dissolved aluminium influences the stability some drops of the aluminium sample tubes named above were added to the SA mixture of 44 wt% of water after the second triggering experiment. The expected rise of temperature where homogenous crystallisation sets in did not show. Instead the temperature dropped. Neither the expectation that temperature of homogenous nucleation is correlated with the way of melting or cooling could be confirmed. Another explanation for results with different temperatures could be done by assuming different contact between thermocouple and Peltier element. Thus further investigations have to be done to possibly find any correlations.

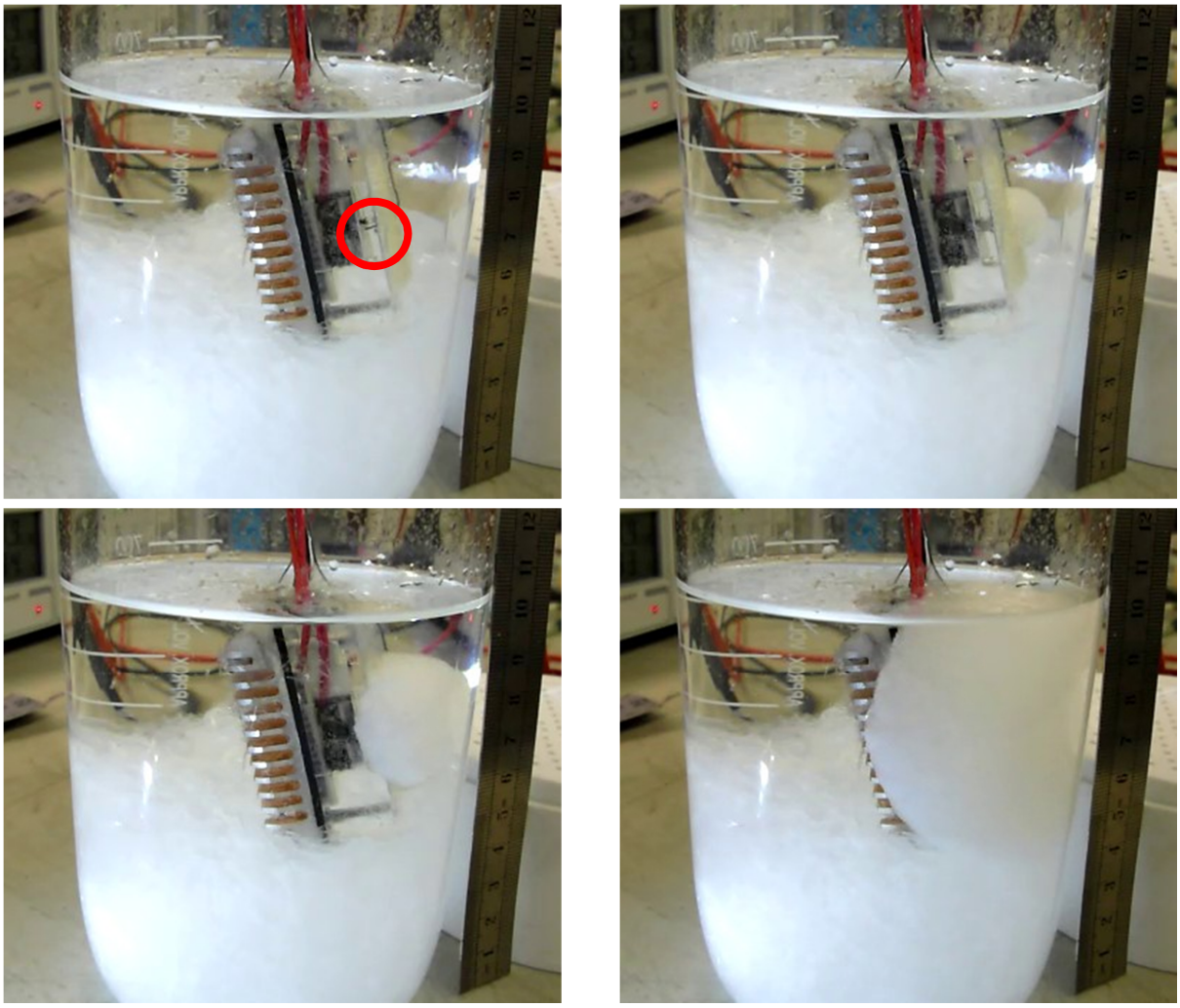

Figure 3-25: Snapshots of the crystallisation progress with ca. 2 · s timestep. The circle in the first picture marks the cavity at the "cold side" of the Peltier-element before start of crystallisation.

3.5.3 Investigation of h/T-characteristics for PCM

This chapter is used to discuss the obtained results of h/T-characteristics for the two investigated SA mixtures of 42 · wt% and 44 · wt% of water respectively and to give an estimation of errors of the measurement method. A discussion of the Biot number, Bi, during a measurement cycle is followed by the presentation and discussion of the finally received h/T-correlations.

The control of Bi, has to be done to verify the assumption of spatially uniform temperature within the sample. Bi is calculated exemplarily for one sample in one reference measurement cycle for all time steps of the experiment by equation 3-6. Bi is plotted against the time scale of the experiment which is shown in figure 3-26 and 3-27 respectively.

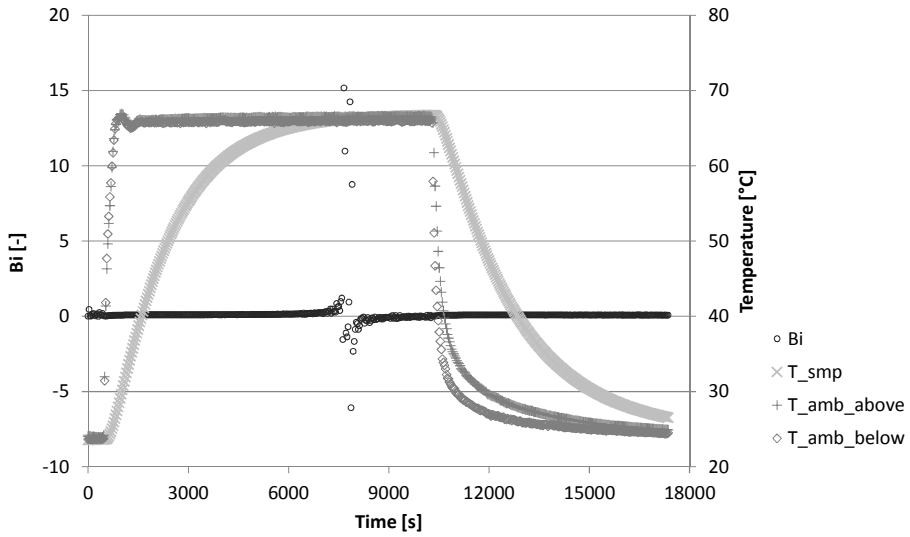

Figure 3-26: Evalutaion of the Biot number, Bi, with time is shown for one reference measurement with water. High values of Bi result from errors in temperature measurement of the ambient. Figure 3-27 shows Bi and the temperatures in a bigger scale.

The two figures are only different in the scale of Bi and the temperature. The first one shows very well that Bi is almost constant during the whole experiment. The strong rise in Bi in the middle of figure 3-26 is caused by very small temperature differences $\Delta T_{amb,smp}$ which cause high values of Bi as long as the transferred heat is not zero. The negative values are caused by higher temperature in the sample than ambient on one hand and still positive $\dot{Q}_{conv}$ on the other. Theoretically this is not possible and it shows an error in measurement of the ambient temperature in the drying oven. Calibration of the used thermocouples gave an accuracy of about $\pm 0.03 \cdot K$ in the experiments with water and where considered as sufficient. It is assumed that the error results from unpredictable fluctuations due to strong convection in the drying oven. Nevertheless in this area the heat transfer rates are very small and a uniform sample temperature can be assumed. Figure 3-27 shows that for the rest of the measurement $Bi < 0.1$ is given. Thus the assumption of uniform temperature within the sample was correct.

s

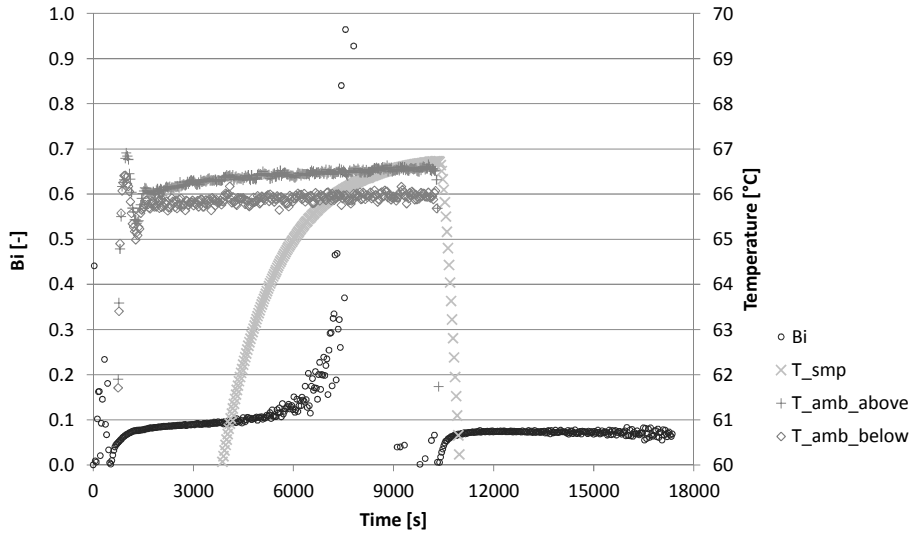

Figure 3-27: Evalutaion of the Biot number, Bi, with time is shown for one reference measurement with water. High values of Bi result from errors in temperature measurement of the ambient. Figure 3-26 shows Bi and the temperatures in a smaler scale.

Figure 3-28 to 3-30 finally show all h/T-characteristics obtained by the measurements with SA mixtures. Figure 3-29 and figure 3-30 show the results of three measurement runs with SA mixtures of 42 · wt% and of 44 · wt% water respectively Two samples were investigated for each concentration. Figure 3-28 is used as representative sample to discuss the obtained h/T-curves. It is the same sample as given by the curve 44a_run2 in figure 3-30.

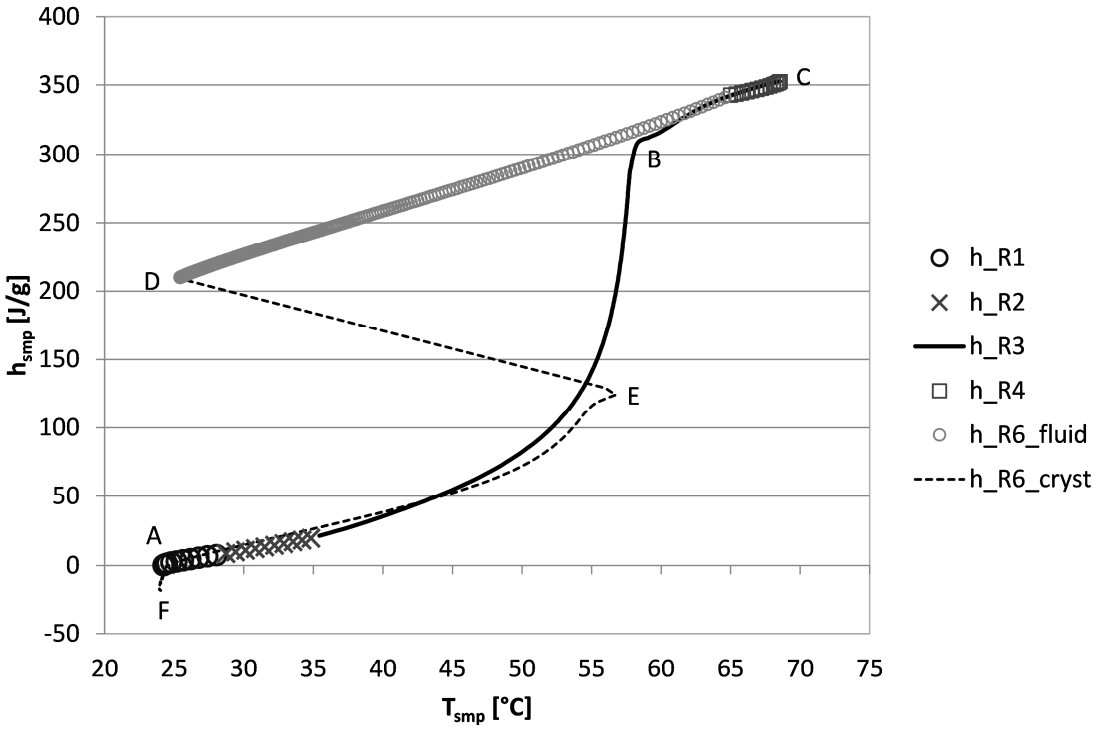

Figure 3-28: Representative h/T-characteristic for sample 44a, run2 with different symbols for the ranges as defined in section 3.4

In the following section the whole measurement cycle of heating, undercooling to ambient temperature, crystallisation and cooling to ambient again will be discussed in detail and related to observations of segregation, steps in the phase diagram and possible failure of the measurement method. The curve in figure 3-28 is used for demonstration. The evolution of h_{smp} is marked with letters A to F for a better description of the steps in the experiment. The measurement starts at point A with a crystalline SA mixture sample at about 25 °C at ambient air. The curve A to C gives the heating phase of the experiment. At the beginning of heating the enthalpy of the sample, h_{smp}, is set zero and rises almost linearly. Linearity can be related to almost constant specific heat, c_p, of the investigated SA mixture in the solid state. When phase change sets in, the linear correlation between T_{smp} and h_{smp} changes into a curve because phase change enthalpy of fusion, $\Delta_{fus}h$, is taken into account and h_{smp} rises not only by c_p but $\Delta_{fus}h$ as well.

The problem of measurement of c_p shows up. Evaluation of c_p is only possible if distinction of the contribution of c_p and $\Delta_{fus}h$ to h_{smp} is possible. This distinction is only possible when the ratio of material that is molten in each time step of evaluation is known. This information can only be received if the ratio of solid to liquid would be measured which was never accounted for in this experimental method. Three theoretical possibilities to receive estimated values for c_p of solid PCM would be firstly to relate the ratio of solid to liquid to reaction (melting) rates, secondly to obtain the ratio of solid to liquid out of equilibria between solid and liquid from the phase diagram or thirdly to evaluate only the linear interval of obtained h/T-curves assuming that no solid is molten in this interval. The second method is only a theoretical attempt because the time to reach equilibrium at different temperatures during the measurements can be assumed to be too short to reach equilibrium state during measurements. Thus measurement of c_p for solid SA mixtures is not easy. For numerical modelling the obtained h/T-correlation should give all the needed information of capability of investigated PCM to store a certain amount of heat.

Coming back to the h/T-curve in figure 3-28 the shape changes to linear correlation in point B of the heating period again. Theoretically the lines between B-C and C-D should coincide exactly because when all solid is molten only c_p contributes to h_{smp}. This is not shown in figure 3-28. An explanation for this result is that equilibrium is not reached at point B. Thus some solids remain in the sample and get molten during further heating to point C which gives a greater slope of the h/T-curve for the interval B-C due to an additional amount of $\Delta_{fus}h$ besides c_p to h_{smp}. It can be assumed that after point B no solid SAT exists in the sample mixture but SA because SAT is not stable above 58 · °C as discussed in chapter 2.1. Therefore the extra Δh should correctly not be named $\Delta_{fus}h$ but $\Delta_{sol}h$ for enthalpy of dissolution. Furthermore for undercooling to room temperature along line B to C the same but inverse effect is expected for samples with 42 · wt% at about 35 °C according to the discussion in chapter 3.5.2 due to precipitation of SA or so called segregation. This effect is not observed for any of the measured h/T-courses. The only explanation for this result is, that not all SA is dissolved which has been observed and discussed in chapter 3.5.2 as well. Only shaking dissolves all SA in the vessel. The change in slope for the interval B-C due to $\Delta_{sol}h$

can be observed for the curve B-C because the high temperature forces some SA to dissolve but during cooling the precipitation propagates over a longer period of time and gives no visible change in slope in the measured h/T-trend. This was observed in segregation experiments as well for solutions of 42 wt% water without slewing where no change in slope of T/t-curves was obtained.
The next step to discuss is crystallisation which is represented in the h/T-course by the interval D-E. The great change of roughly $80 \cdot J \cdot g^{-1}$ (corresponding to roughly 900 J for the whole sample) in h_{smp} within one time step of 31 s can be explained by the thermal mass of the steel sample tube. Equation 3-5 gives the final step in calculation of Δh_{smp}. The high value of ΔT_{smp} in the first time step after crystallisation results from the difference between room temperature and the melting temperature. It is assumed for the whole measurement that the temperatures within the whole sample and sample tube are uniform and therefore the measured sample temperature can be used to calculate enthalpy changes of the steel sample tube. The high value of ΔT_{smp} implies that all the heat needed to bring the tube to melting temperature is released by the PCM in this single time step. Therefore this term of equation 3-5 gets very negative and increases the calculated negative amount of Δh_{smp} additional to the relative strong negative value of $\dot{Q}_{conv}$ that is given for this time step anyway due to the high value of $\Delta T_{amb,smp}$.
The last part of the h/T-curve, E-F represents the cooling to room temperature. It coincides almost with line E-A which should be correct for lower temperatures because the vast amount of the material should be solid again and therefore only c_p of the solid material should contribute in the change of h_{smp}. Theoretically the first part of E-F should start at lower temperatures than depicted because if the sample steel tube would have the same temperature as the PCM the roughly 900 J for heating it up are used from the heat of fusion which should result in a lower temperature of the sample than the melting temperature. In fact the temperature drops from the initial melting temperature within a lag of a few minutes as shown in figure 3-31. Therefore the measured T_{smp} in the initial phase of evaluation is not correct. This results in a $\dot{Q}_{conv}$ that is too high for the first time steps. Additionally the temperature of the insulation surface will be lower in the initial phase than afterwards when a steady state is reached which leads to higher values of $\dot{Q}_{conv}$ in evaluation than in the actual experiment again. On the other hand the thermal mass of the insulation that needs to be heated up compensates this failure. To summarize, for step E to F additional work needs to be done to get more accurate results but it can be assumed that only a short initial phase will have an unpredictable small error.

The different symbols for the h/T-correlation in figure 3-28 correlate to the intervals of evaluation. Since along the whole h/T-course no strong change at the limit between two evaluation intervals occurs it can be assumed that besides the well-defined areas of $\dot{Q}_{conv}$ ($\Delta T_{amb,smp}$) the approximation to the hysteresis was well performed.
Also the result that h_{smp} after a complete experimental cycle meets a value of zero again is an indicator for no big systematic error.

In figures 3-29 and 3-30 the data of one complete run with melting, undercooling and crystallisation with subsequent cooling is shown. The curves named run1 represent the crystallisation part (the start value for h_{smp} is the mean of the samples with same concentration in their undercooled state), curves with run2 are complete and run3 represents only heating with most of the part of undercooling. The values are for all measurements within the same accuracy level. The difference between samples with same concentration are higher for samples with 42 wt% water. An explanation for this could be segregation because samples with 44 wt% of water should show almost no segregation and have therefore the better correlation.

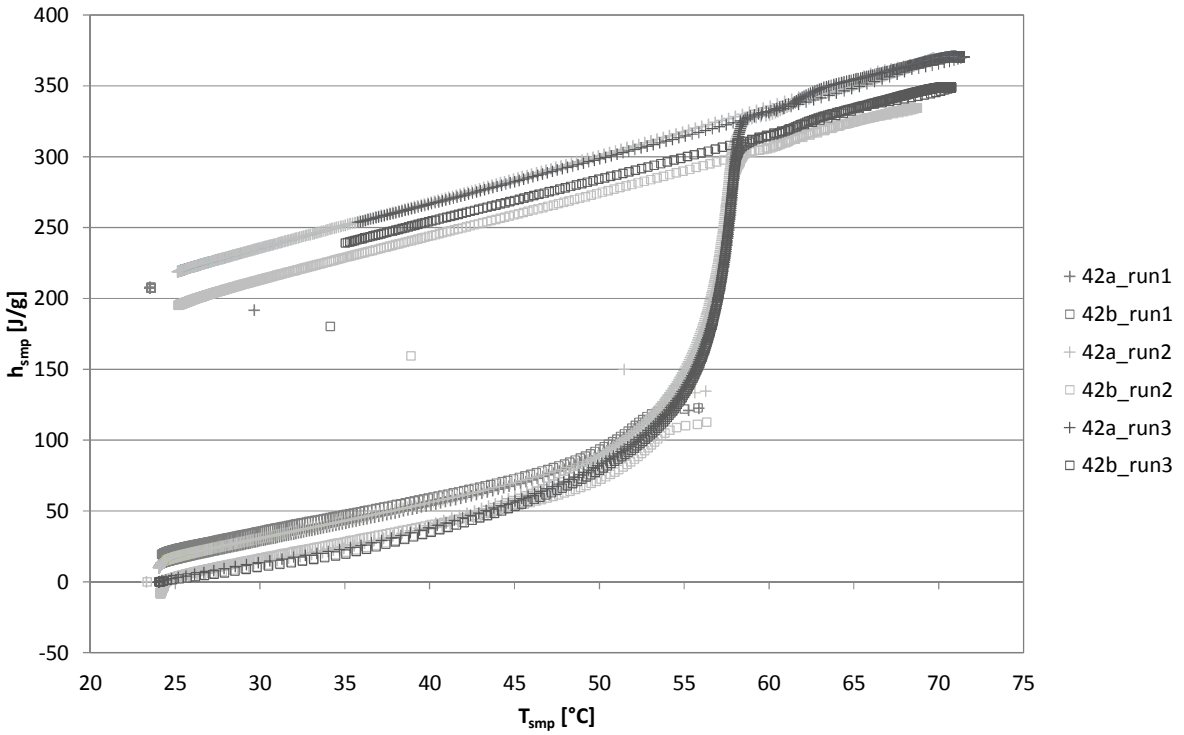

Figure 3-29: h/T-characteristic for different samples (a,b) with 42 wt% water

As mentioned above the measurements have been stopped with the steel tubes because a system that is not completely closed is always a source for crystallisation seeds on one hand and it is not predictable how much weight during a measurement is lost on the other hand. Especially during measurements with the investigated SA mixtures the rubber plug has to be removed for each crystallisation and cannot be plugged in as tight as after initial filling because the sample tubes are assembled in the box. The T-shape of the steel tube is probably not optimal because it has to be fixed in a way that the side piece is in vertical position because otherwise the SA mixture would get in contact with the sealing plug and probably leak. The vertical arrangement leaves the side piece always in lee direction of air movement of the tube where the amount depends on how strictly vertical the tube is mounted. If a little tilt occurs a different surface area is exposed to the air stream from below. Since only the lower part of the steel tube is filled with sample material the assumed uniform temperature of sample and tube is then not given.

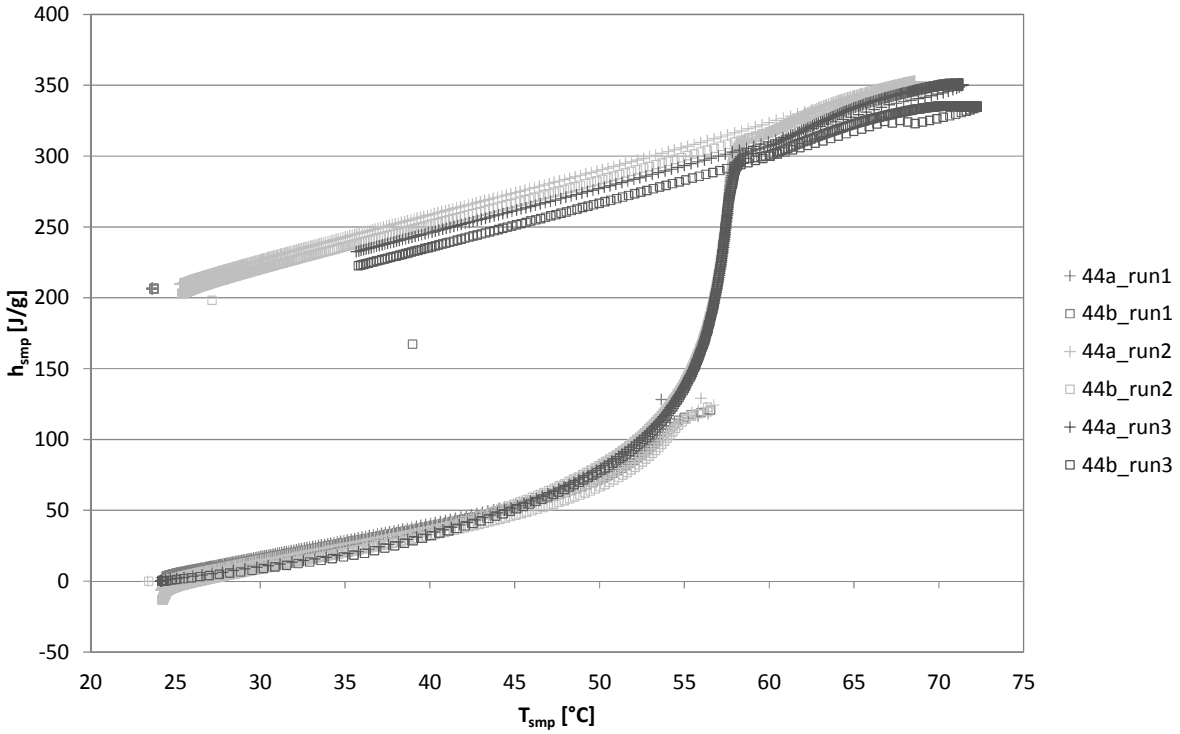

Figure 3-30: h/T-characteristic for different samples (a,b) with 44 wt% water

Having the different temperature trends of figures 3-21 and 3-23 in mind one can conclude from figure 3-31 that no segregation occurred in samples B2 and B3 and hence no segregation effects appear in figures 3-29 and 3-30.

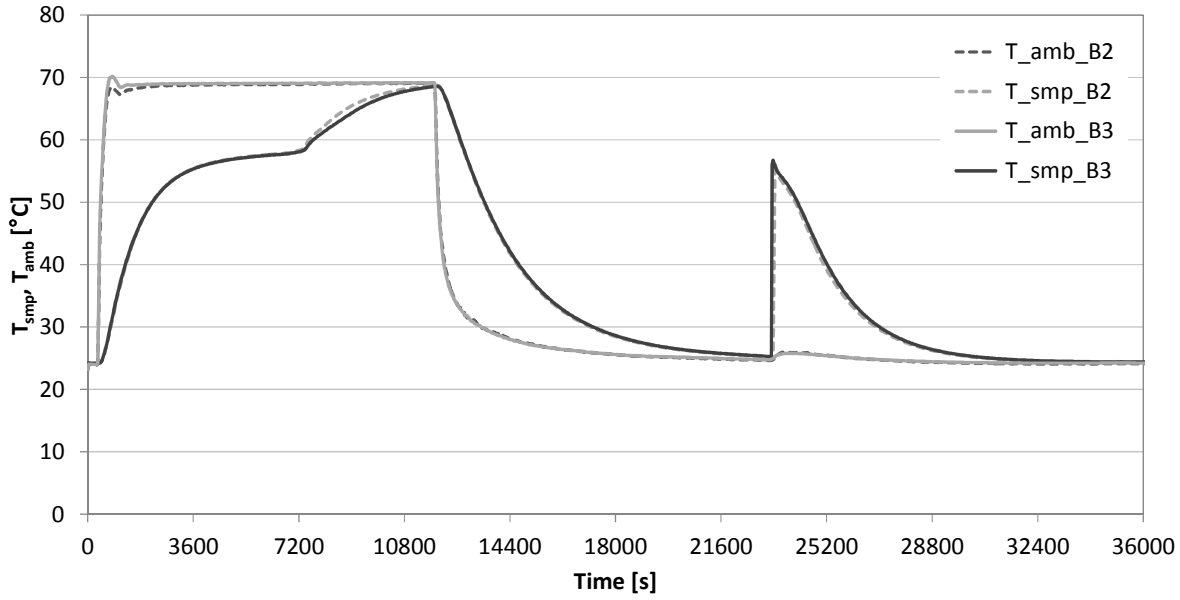

Figure 3-31: Temperature time trend of a typical measurement with a sample with 42 wt% water (B2) and 44 wt% water (B3) respectively.

4 SUMMARY AND CONCLUSIONS

The aim of this work was to characterise the chemical system of sodium acetate / water and establish a measuring method for determination of the enthalpy/temperature-characteristic with special regard to undercooling and controlled crystallisation. Additionally experiments for investigation of segregation were performed.

Stability of undercooling is strongly related to almost completely filled vessels where the possibility for a drop to dry out during melting is very low. Wetting is a huge problem for vessel sealings. Experiments with an apparatus to test crystallisation gave the result that SA mixtures are able to leak through a paper sealing and causes crystallisation during cooling through the paper sealing. The best way to close a vessel is to use a PTFE sealing because it's strongly hydrophobic and it gave the best results. Stability of undercooled SAT is more critical than for dilute mixtures but if the vessel is sealed in properly undercooling should not be a problem. Another observation during tests of triggering crystallisation was that vessels with a large amount of surfaces that touch each other like screws do not show stable undercooling like SA mixtures in glass vessels.
Tests for triggering crystallisation were only successful through seeding and with a Peltier unit. A mechanical device that causes crystallisation by seeding was built and successfully tested. It can be used to trigger crystallisation in T-History experiments.

The experimental results of investigation of h/T-characteristics are too small in sample size to give a statement about reliability of the measurement method. But the results correlate well with literature data and deliver physically meaningful results. Further improvements of the sample tubes and temperature measurement of the ambient air have to be done.

Segregation experiments show very good correlation with the phase diagram. For SA mixture samples with less than 44 wt% of water segregation has appeared in almost all samples and even samples of 44 wt% of water show segregation in some cases. Samples with 42 wt% of water show segregation without exception. Segregation showed no correlation to filling height of a sample tube. To definitely avoid segregation a minimum of 45 wt% of water can be recommended from observations.

SYMBOLS

Bi	Biot number
$c_{p,i}$	Heat capacity at constant pressure for a substance i
G	Gibbs energy
ΔG	Change of Gibbs energy
$\Delta_{fus}h$	Phase change enthalpy of fusion
$\Delta_{sol}h$	Enthalpy of solution
Δh_{smp}	Change in specific enthalpy of a sample during a measurement interval
ΔH	Change in enthalpy of sample and sample tube during a measurement interval
$\left(\frac{\partial G}{\partial T}\right)_p$	Partial derivative of Gibbs energy with respect to time at constant pressure
m_i	Mass of a component i
PC	Personal computer
$\dot{Q}$	Heat exchange rate during a time interval
S	Entropy
Δt	Time interval of a measurement step
T	Temperature
T_{amb}	Ambient temperature for a sample tube during measurements
T_{smp}	Temperature of the sample during measurements
ΔT_{smp}	Temperature difference of the sample in a considered timeintervall
$\Delta T_{amb,smp}$	Temperature difference between ambient and sample
r	Radius of nucleus and cluster respectively
W()	Mass concentration of a substance in wt%
σ	Surface tension of the nucleus in the parent phase
λ	Thermal conductivity

ABBREVIATIONS

COMTES	Combined development of compact thermal energy storage technologies: project number 295568
DSC	Differential scanning calorimeter
EeB	Energy-efficient Buildings
EU	European Union
h/T – progress	(Specific) enthalpy/temperature – progress
IWT	Institute of Thermal Engineering (Institut für Wärmetechnik)
PCM	Phase change material
PPP	Public Private Partnership
SA	Sodium acetate
SAT	Sodium acetate trihydrate
T/t-curves	Progress of temperature with time during heating or cooling of a SA mixture
TES	Thermal energy storage
T-History-Method	Temperature History Method
wt%	Per cent by weight

REFERENCES

[1] Sandnes B., Exergy Efficient Production, Storage and Distribution of Solar Energy, PhD thesis, 2003, University of Oslo

[2] European Commission - Eurostat, Final energy consumption, by sector, 2010, http://epp.eurostat.ec.europa.eu/tgm/graph.do?tab=graph&plugin=1&pcode=tsdpc320&language=en&toolbox=sort, [Access 12-09-30].

[3] Ad-hoc Industrial Advisory Group, Energy-efficient Buildings PPP, 2010, http://ec.europa.eu/research/industrial_technologies/pdf/ppp-energy-efficient-building-strategic-multiannual-roadmap-info-day_en.pdf, [Access 12-09-30].

[4] European Commission - Eurostat, Share of renewable energy in gross final energy consumption - %, 2010, http://epp.eurostat.ec.europa.eu/tgm/graph.do?tab=graph&plugin=1&pcode=tsdcc110&language=en&toolbox=data, [Access 12-09-30]

[5] Heinz A., Application of Thermal Energy Storage with Phase Change Materials in Heating Systems, PhD thesis, 2007, Graz University of Technology

[6] Schultz J. M., Furbo S., Solar heating systems with heat of fusion storage with 100% solar fraction for solar low energy buildings, Proceedings of ISES world congress 2007 (Vol. I – Vol. V), Beijing, China

[7] Furbo S., Heat storage with an incongruently melting salt hydrate as storage medium based on the extra water principle, Report 108, 1980, Technical University of Denmark

[8] Fan J., Furbo S., et al., Thermal behaviour of a heat exchanger module for seasonal heat storage, Energy Procedia, SHC 2012

[9] Cabeza L., Heinz A., et al., Inventory of Phase Change Materials (PCM), Report C2 of Subtask C of IEA Solar Heating and Cooling programme – Task 32 "Advanced storage concepts for solar and low energy buildings", 2005

[10] Araki N., Futamura M., et al., Measurements of Thermophysical Properties of Sodium Acetate Hydrate, International Journal of Thermophysics, Vol. 16, No. 6, 1995, p. 1455-1465

[11] Wada T., Yamamoto R., Studies on Salt Hydrate for Latent Heat Storage. I. Crystal Nucleation of Sodium Acetate Trihydrate Catalyzed by Tetrasodium Pyrophosphate Decahydrate, Bul. Chem. Soc. Jpn., 55, 1982, p. 3603-3606

[12] Lane G .A., Solar Heat Storage: Latent Heat Materials, 1986, CRC Press, Inc., Florida

[13] Meyer R. J., Pietsch E.E., Gmelins Handbuch der Anorganischen Chemie, 1967, system number 21, supplementary volume 4, Verlag Chemie GmbH, Weinheim

[14] Mitchell M., Engauge Digitizer - Digitizing software, 2012.
downloaded from http://digitizer.sourceforge.net/ [Access 29-09-29]

[15] Gmelins Handbuch der Anorganischen Chemie, 1928, system number 21, Verlag Chemie GmbH, Berlin

[16] Atkins P. W., Physical Chemistry, 1999, Oxford University Press, Oxford

[17] Dunning W. J., Walton A. G., et al., Nucleation, 1969, Marcel Dekker, Inc., New York

[18] Springer Materials The Landolt-Börnstein Database,
http://www.springermaterials.com/docs/pdf/978-3-540-44760-3_115.html?queryterms=%22x6crnimoti17%22 [Access 12-09-29]

[19] Tufeu R., Le Neindre B., et al., Thermal Conductivity of Several Liquids, C.R.Hebd.Seanc.Acad.Sci.Ser.B Sci.Phys., 262, 1966, p. 229-231

[20] Ginnings D.C., Furukawa G.T., Heat Capacity Standards for the Range 14 to 1200°K. J.Am.Chem.Soc., 75, 1953, p. 522-527

[21] Holleman A. F., Wiberg E., Wiberg N. [Bearb.], Lehrbuch der Anorganischen Chemie, 2007, 102. stark umgearbeitete und verb. Aufl., de Gruyter, Berlin, New York, p. 1142-1143

APPENDIX

Calibration functions of temperature sensors

Table A-1: Calibration data for temperature sensors (performed on June 19th) and coefficients for a linear calibration function. Refercence sensor: Burster, Kelvimat, type 4303, Pt100

Sensor	Reading points for calibration [°C]	Proportional factor [K^{-1}]	Offset [K]	Reading points for control measurement [°C]	Maximum deviation in control meas. [K]
B1	10, 50, 70, 90	1.0012	-0.0483	40, 50, 70, 90	0.022
B2	10, 50, 70, 90	1.0007	-0.0833	40, 50, 70, 90	0.042
B3	10, 50, 70, 90	1.0009	-0.0423	40, 50, 70, 90	0.030
B4	10, 50, 70, 90	1.0010	-0.0119	40, 50, 70, 90	0.029
TC1	10, 50, 70, 90	1.0024	-0.1317		
TC2	10, 50, 70, 90	1.0022	-0.0585		
TC3	10, 50, 70, 90	1.0024	0.0287		
TC4	10, 50, 70, 90	1.0030	0.0769		
TC5	10, 50, 70, 90	1.0021	-0.0956		
TC6	10, 50, 70, 90	1.0018	-0.0495		
TC7	10, 50, 70, 90	1.0028	-0.0004		
TC8	10, 50, 70, 90	1.0028	0.0758		

Weights

Table A-2: Weights of sample tubes (steel) and filling material for h/T-measurements

Sample	mass of steel [g]	mass of water [g]	mass of SAT [g]
42a	54.7358	7.9757	11.0284
42b	54.8314	8.0283	11.1373
44a	55.5501	8.1174	11.2319
44b	54.5175	7.9940	11.2114

Complete recorded data of h/T measurements

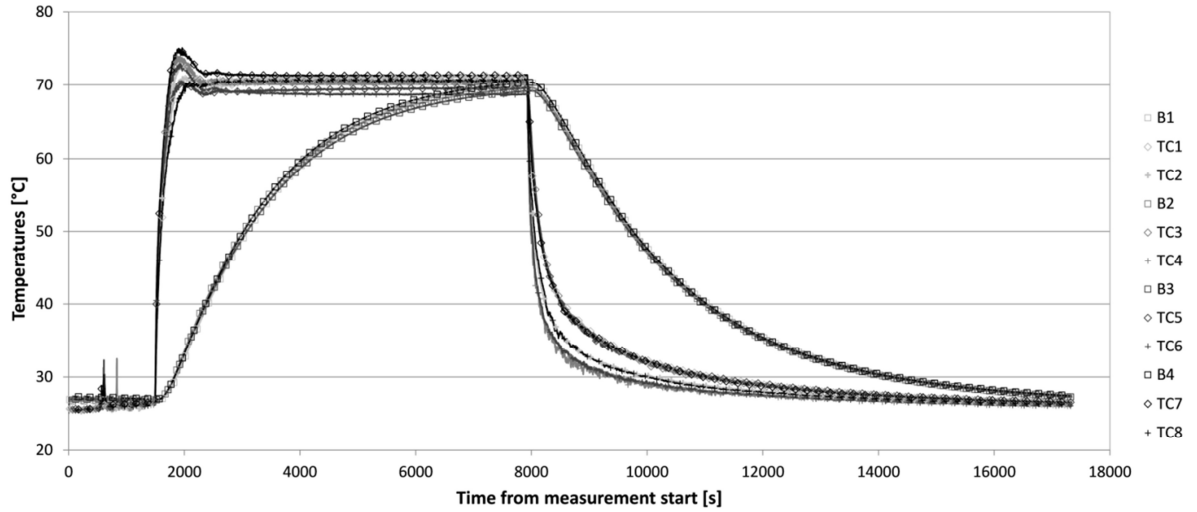

		B1	B2	B3	B4	TC1	TC2	TC3	TC4	TC5	TC6	TC7	TC8
		[°C]	[°C]	[°C]	[°C]	[°C]	[°C]	[°C]	[°C]	[°C]	[°C]	[°C]	[°C]
11.07.2012	14:42:54.000	25.30	25.46	25.57	25.54	25.48	25.20	25.36	25.19	25.48	25.29	25.41	25.25
11.07.2012	14:42:55.000	25.32	25.48	25.57	25.54	25.45	25.20	25.37	25.17	25.48	25.30	25.41	25.27
11.07.2012	14:42:56.000	25.32	25.48	25.58	25.56	25.48	25.18	25.35	25.13	25.48	25.30	25.41	25.26
11.07.2012	14:42:57.000	26.93	26.76	27.01	27.25	25.69	25.64	25.63	25.61	25.68	25.60	25.76	25.64
11.07.2012	14:42:58.000	26.92	26.74	27.00	27.25	25.73	25.65	25.66	25.60	25.70	25.60	25.76	25.61
⋮	⋮	⋮	⋮	⋮	⋮	⋮	⋮	⋮	⋮	⋮	⋮	⋮	⋮
11.07.2012	19:31:48.000	27.22	27.27	27.30	27.48	26.40	26.17	26.46	26.08	26.58	26.08	26.59	26.27

Figure A-1: Complete recorded data for measurements of run 1 with water

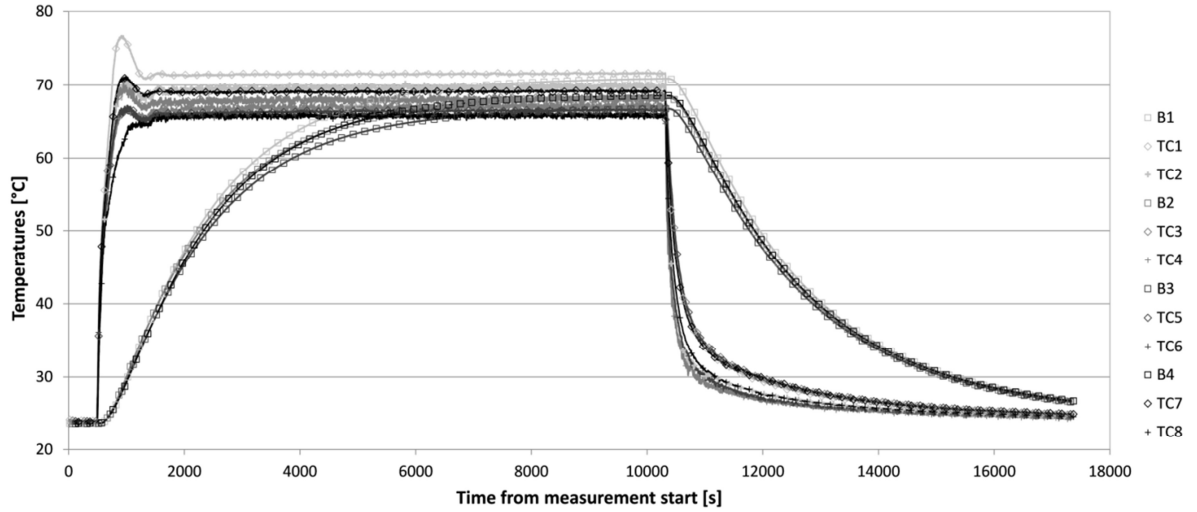

		B1	B2	B3	B4	TC1	TC2	TC3	TC4	TC5	TC6	TC7	TC8
		[°C]	[°C]	[°C]	[°C]	[°C]	[°C]	[°C]	[°C]	[°C]	[°C]	[°C]	[°C]
16.07.2012	14:52:42.000	23.40	23.37	23.39	23.53	23.71	23.27	23.65	23.24	23.73	23.30	23.67	23.21
16.07.2012	14:52:43.000	23.40	23.35	23.38	23.54	23.72	23.29	23.65	23.26	23.73	23.32	23.68	23.22
16.07.2012	14:52:44.000	23.42	23.37	23.38	23.54	23.71	23.28	23.64	23.26	23.73	23.30	23.68	23.22
16.07.2012	14:52:45.000	23.64	23.60	23.58	23.67	24.18	23.68	24.12	23.64	24.12	23.68	23.93	23.69
16.07.2012	14:52:46.000	23.63	23.60	23.56	23.68	24.18	23.68	24.12	23.63	24.12	23.68	23.88	23.68
⋮	⋮	⋮	⋮	⋮	⋮	⋮	⋮	⋮	⋮	⋮	⋮	⋮	⋮
16.07.2012	19:42:44.000	26.57	26.52	26.48	26.71	24.71	24.51	24.80	24.38	24.88	24.48	24.91	24.55

Figure A-2: Complete recorded data for measurements of run 2 with water

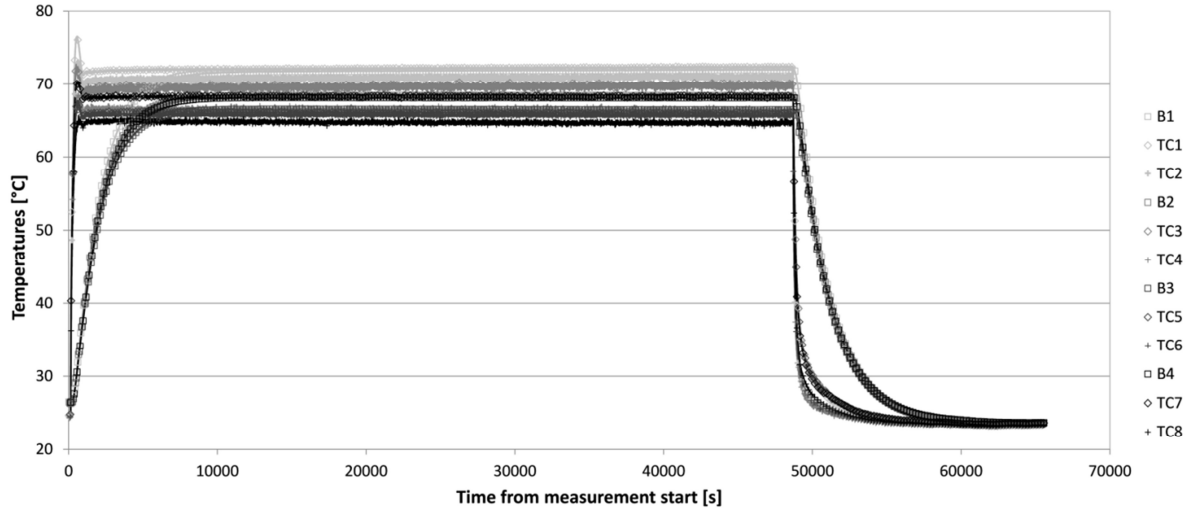

		B1	B2	B3	B4	TC1	TC2	TC3	TC4	TC5	TC6	TC7	TC8
		[°C]	[°C]	[°C]	[°C]	[°C]	[°C]	[°C]	[°C]	[°C]	[°C]	[°C]	[°C]
16.07.2012	19:43:29.000	26.57	26.50	26.50	26.69	24.72	24.51	24.78	24.36	24.88	24.49	24.94	24.55
16.07.2012	19:43:30.000	26.57	26.52	26.50	26.69	24.71	24.51	24.78	24.38	24.88	24.48	24.89	24.54
16.07.2012	19:43:31.000	26.57	26.50	26.50	26.71	24.71	24.51	24.80	24.36	24.87	24.48	24.90	24.55
16.07.2012	19:43:32.000	26.50	26.48	26.45	26.65	24.67	24.50	24.77	24.29	24.88	24.37	24.90	24.54
16.07.2012	19:43:33.000	26.52	26.45	26.45	26.64	24.70	24.50	24.77	24.25	24.86	24.37	24.89	24.55
⋮	⋮	⋮	⋮	⋮	⋮	⋮	⋮	⋮	⋮	⋮	⋮	⋮	⋮
17.07.2012	13:56:55.000	23.43	23.53	23.61	23.72	23.60	23.31	23.58	23.32	23.64	23.39	23.70	23.46

Figure A-3: Complete recorded data for measurements of run 3 with water

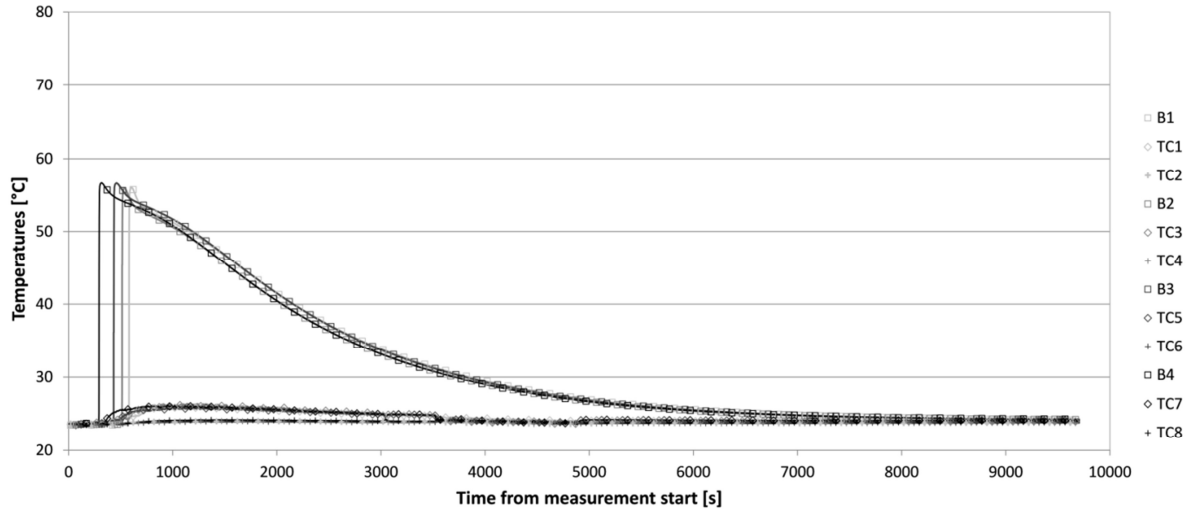

		B1	B2	B3	B4	TC1	TC2	TC3	TC4	TC5	TC6	TC7	TC8
		[°C]	[°C]	[°C]	[°C]	[°C]	[°C]	[°C]	[°C]	[°C]	[°C]	[°C]	[°C]
19.07.2012	09:44:11.000	23.50	23.56	23.62	23.72	23.62	23.45	23.65	23.47	23.72	23.47	23.73	23.53
19.07.2012	09:44:12.000	23.50	23.55	23.61	23.72	23.62	23.45	23.66	23.46	23.70	23.48	23.73	23.52
19.07.2012	09:44:13.000	23.50	23.55	23.62	23.72	23.62	23.45	23.66	23.46	23.73	23.47	23.73	23.52
19.07.2012	09:44:14.000	23.52	23.58	23.64	23.74	23.62	23.45	23.64	23.46	23.70	23.47	23.72	23.50
19.07.2012	09:44:15.000	23.51	23.56	23.64	23.74	23.62	23.43	23.64	23.46	23.72	23.47	23.71	23.50
⋮	⋮	⋮	⋮	⋮	⋮	⋮	⋮	⋮	⋮	⋮	⋮	⋮	⋮
19.07.2012	12:25:54.000	24.20	24.23	24.25	24.31	24.04	23.83	24.00	23.81	24.11	23.84	24.15	23.91

Figure A-4: Complete recorded data for measurements of run 1 with SAT

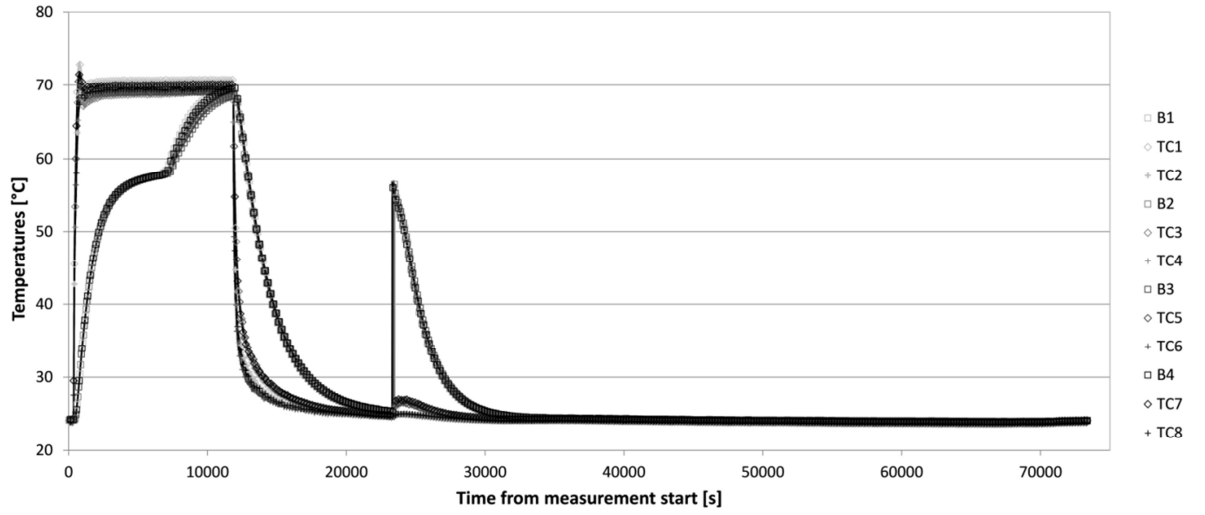

		B1	B2	B3	B4	TC1	TC2	TC3	TC4	TC5	TC6	TC7	TC8
		[°C]	[°C]	[°C]	[°C]	[°C]	[°C]	[°C]	[°C]	[°C]	[°C]	[°C]	[°C]
19.07.2012	12:28:23.000	24.19	24.25	24.23	24.31	24.04	23.86	24.03	23.85	24.16	23.90	24.18	23.94
19.07.2012	12:28:24.000	24.18	24.23	24.23	24.30	24.08	23.86	24.06	23.86	24.17	23.91	24.18	23.96
19.07.2012	12:28:25.000	24.19	24.23	24.25	24.30	24.07	23.88	24.06	23.86	24.16	23.91	24.19	23.96
19.07.2012	12:28:26.000	24.18	24.23	24.25	24.31	24.08	23.87	24.06	23.86	24.17	23.91	24.20	23.97
19.07.2012	12:28:27.000	24.19	24.23	24.23	24.30	24.08	23.86	24.03	23.85	24.16	23.90	24.18	23.95
⋮	⋮	⋮	⋮	⋮	⋮	⋮	⋮	⋮	⋮	⋮	⋮	⋮	⋮
20.07.2012	08:52:36.000	23.90	23.98	24.06	24.14	24.07	23.78	23.99	23.77	24.14	23.79	24.15	23.89

Figure A-5: Complete recorded data for measurements of run 2 with SAT

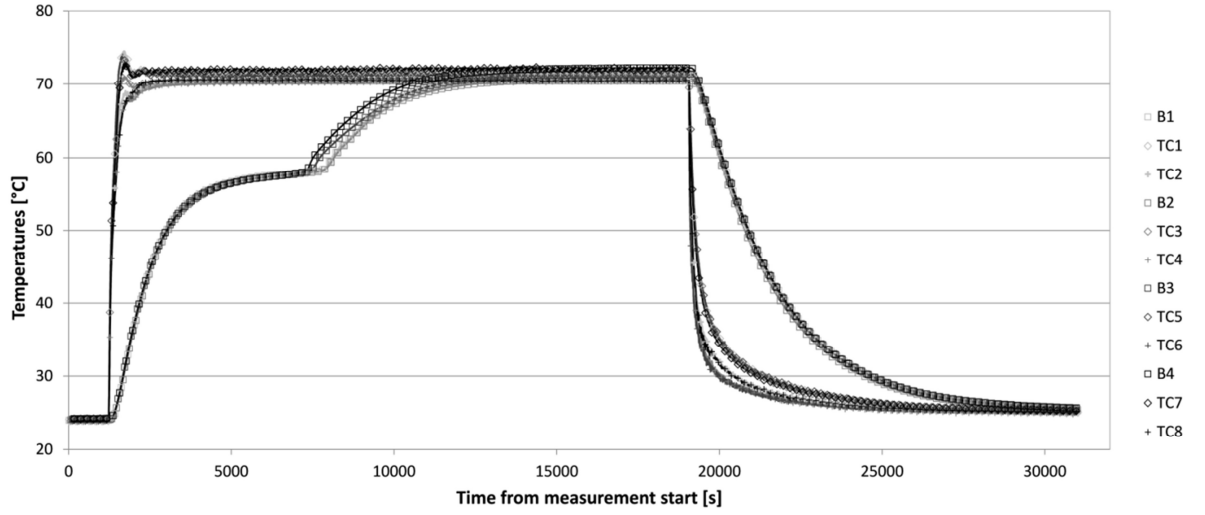

		B1	B2	B3	B4	TC1	TC2	TC3	TC4	TC5	TC6	TC7	TC8
		[°C]	[°C]	[°C]	[°C]	[°C]	[°C]	[°C]	[°C]	[°C]	[°C]	[°C]	[°C]
20.07.2012	09:12:58.000	24.01	24.09	24.15	24.25	24.13	23.82	24.07	23.82	24.16	23.86	24.22	23.97
20.07.2012	09:12:59.000	24.02	24.08	24.15	24.25	24.11	23.82	24.06	23.80	24.18	23.87	24.22	23.97
20.07.2012	09:13:00.000	24.01	24.07	24.15	24.25	24.13	23.82	24.06	23.82	24.17	23.86	24.21	23.95
20.07.2012	09:13:01.000	24.03	24.10	24.15	24.25	24.13	23.80	24.04	23.82	24.16	23.85	24.21	23.96
20.07.2012	09:13:02.000	24.02	24.07	24.15	24.27	24.11	23.81	24.06	23.80	24.16	23.86	24.21	23.95
⋮	⋮	⋮	⋮	⋮	⋮	⋮	⋮	⋮	⋮	⋮	⋮	⋮	⋮
20.07.2012	17:50:33.000	25.42	25.43	25.57	25.67	25.14	24.94	25.10	24.87	25.22	24.99	25.22	25.05

Figure A-6: Complete recorded data for measurements of run 3 with SAT